

**CASE FILE  
COPY**

**THE EFFECT OF ALLOYING ON GAMMA AND  
GAMMA PRIME IN NICKEL-BASE SUPERALLOYS**

**R.L. Dreshfield and J.F. Wallace**

**CASE WESTERN RESERVE UNIVERSITY**

**prepared for**

**NATIONAL AERONAUTICS AND SPACE ADMINISTRATION**

**NASA Lewis Research Center**

**GRANT NGR 36-027-019**

1. Report No. NASA CR-120940		2. Government Accession No.		3. Recipient's Catalog No.	
4. Title and Subtitle THE EFFECT OF ALLOYING ON GAMMA AND GAMMA PRIME IN NICKEL-BASE SUPERALLOYS				5. Report Date May, 1972	
				6. Performing Organization Code	
7. Author(s) R.L. Dreshfield and J.F. Wallace				8. Performing Organization Report No.	
9. Performing Organization Name and Address Case Western Reserve University 10900 Euclid Avenue Cleveland, Ohio 44106				10. Work Unit No. 134-03-20	
				11. Contract or Grant No. NGR-36-027-019	
12. Sponsoring Agency Name and Address National Aeronautics and Space Administration Washington, D.C. 20546				13. Type of Report and Period Covered Contractor Report July 70 to May 72	
				14. Sponsoring Agency Code	
15. Supplementary Notes Project Manager, Richard L. Ashbrook, Materials and Structures Division, NASA Lewis Research Center, Cleveland, Ohio 44135					
16. Abstract  An investigation was conducted to determine the compositional limits of $\gamma$ and $\gamma'$ phases in nickel-base superalloys. Fifty-one nickel-base alloys were melted under vacuum and heat treated for 4 hours at 1190°C followed by 1008 hours at 850°C. The alloys had the following composition ranges; Al 4.0 to 13 atomic %, Cr 6.5 to 20.5%, Ti 0.25 to 4.75%, Mo 0.0 to 6.0% and W 0.0 to 4.0%. The residues from the ammonium sulfate electrolytic extraction for the two phase alloys were analyzed chemically and by X-ray diffraction.  The results of the investigation were used to assemble a mathematical model of the $\gamma - \gamma'$ region of the Ni-Al-Cr-Ti-Mo-W system. A computer program was written to analyze the model of the phase diagram. Some of these results are also presented graphically.  The resulting model is capable of satisfactorily predicting the compositions of conjugate $\gamma - \gamma'$ phases in the alloys investigated and twelve of fifteen commercial superalloys studied.					
17. Key Words (Suggested by Author(s)) Metallurgy Superalloys Nickel Alloys Phase Diagram				18. Distribution Statement  Unclassified - unlimited	
19. Security Classif. (of this report) Unclassified		20. Security Classif. (of this page) Unclassified		21. No. of Pages 135	22. Price* \$3.00

\* For sale by the National Technical Information Service, Springfield, Virginia 22151

TABLE OF CONTENTS

	Page
Title Page . . . . .	i
Abstract . . . . .	ii
TABLE OF CONTENTS . . . . .	iii
SUMMARY . . . . .	v
I INTRODUCTION . . . . .	1
II BACKGROUND . . . . .	4
Phase Diagrams . . . . .	4
Published diagrams . . . . .	4
Phase chemistry . . . . .	6
Phase chemistry estimation . . . . .	7
Lattice Mismatch . . . . .	8
Ordering in Gamma Prime . . . . .	11
Occurrence of Other Phases . . . . .	13
Summary Remarks . . . . .	14
III EXPERIMENTAL PROCEDURES . . . . .	16
Selection and Preparation of Alloys . . . . .	16
Heat Treatment . . . . .	18
Location of Test Specimens . . . . .	19
Metallography . . . . .	19
Extraction of Phases . . . . .	20
Chemical Analysis . . . . .	22
X-ray Diffraction . . . . .	23

	Page
Identification of phases . . . . .	23
Lattice parameters . . . . .	24
Relative intensities . . . . .	25
Other Measurements . . . . .	26
Density measurements . . . . .	26
Gamma prime volume . . . . .	26
IV RESULTS AND DISCUSSION . . . . .	27
Gamma Prime Composition . . . . .	27
Amount of Gamma Prime . . . . .	29
Gamma Composition . . . . .	33
Gamma - Gamma Prime Relationships.. . . .	34
Lattice Parameters of Gamma and Gamma Prime . . . . .	43
Degree of Order in Gamma Prime . . . . .	45
Occurrence of Other Phases . . . . .	47
Morphology of Phases . . . . .	50
Gamma and gamma prime . . . . .	50
Additional phases . . . . .	52
Application to Commercial Alloys . . . . .	54
V SUMMARY AND CONCLUSIONS . . . . .	60
REFERENCES . . . . .	64
TABLES . . . . .	71
FIGURES . . . . .	99
APPENDIX . . . . .	120
DISTRIBUTION LIST . . . . .	125

## SUMMARY

The purpose of this investigation was the establishment of compositional limits for the  $\gamma$  and  $\gamma'$  phases of nickel-base superalloys. Fifty-one of these nickel-base alloys were melted and heat treated for 4 hours at 1190°C followed by 1008 hours at 850°C. The alloys had the following composition ranges; Al 4.0 to 13 atomic %, Cr 6.5 to 20.5%, Ti 0.25 to 4.75%, Mo 0.0 to 6.0% and W 0.0 to 4.0%. Electrolytic extractions were performed on the aged alloys using HCl in methanol and ammonium sulfate and citric acid in water as electrolytes. The residues from the ammonium sulfate electrolytic extraction for the two phase alloys were analyzed chemically and by X-ray diffraction.

The results of the experimental determination of composition indicated that  $\gamma'$  varied from 72.1 to 78 atomic % Ni, 7.8 to 17.5% Al, 1.5 to 8.9% Cr, 0.3 to 13.9% Ti, 0.0 to 3.9% Mo and 0.0 to 7.2% W. The composition of  $\gamma$  varied from 1.9 to 15.4 atomic % Al, 6.6 to 30.7% Cr, 0.0 to 3.1% Ti, 0.0 to 8.7% Mo and 0.0 to 5.0% W.

The  $\gamma$  and  $\gamma'$  hypersurfaces were fitted with an equation of the 3rd degree. A computer program was written which can calculate the composition of the conjugate  $\gamma$

and  $\gamma'$  from the composition of a two phase alloy. The program first finds the direction numbers of a tie line from the composition of the alloy, then locates the intersection of the tie line and the solvus hypersurfaces. The results of this calculation compared well with the the experimental results of this investigation and for at least one phase from 15 commercial Ni-base superalloys.

The lattice parameters of  $\gamma$  and  $\gamma'$  were correlated to the phase compositions through simple linear equations. The  $\gamma'$  lattice parameters from commercial Ni-base superalloys were similarly correlated with the  $\gamma'$  composition.

Phases other than  $\gamma$  and  $\gamma'$  were identified in some of the experimental compositions. The phases identified were sigma, mu, Cr solid solution and Mo-W solid solution. The occurrence of these phases was related to the amount of Ni in the alloy, the quantity  $\text{Cr} + 1.75 (\text{Mo} + \text{W})$  in the  $\gamma$ , and the change in Al relative to the change in Cr along the  $\gamma - \gamma'$  tie line. These same parameters appeared to be capable of being adapted for use with commercial Ni-base superalloys.

## I INTRODUCTION

In three decades gas turbines have developed from being a power plant only potentially useful for high performance military aircraft to their current important role in our economy. In addition to their several military roles, gas turbines today are used for commercial air transportation; as an important source of peak load electric power for cities; to pump natural gas to cities; and as a power plant for trains. Much of the success in developing the gas turbine as a viable power plant in our economy can be traced to the development of a family of alloys called superalloys.

The superalloys are iron, nickel, or cobalt-base alloys which are capable of retaining useful strength at elevated temperatures (650° C). The nickel-base superalloys have been developed to the point where they have useful strength to approximately 80% of their melting point.<sup>1\*</sup> Over 50 such alloys are commercially available in this country.

A typical nickel-base superalloy is an alloy containing nickel, aluminum, chromium, carbon, titanium, and boron. In addition molybdenum, tungsten, niobium, tantalum and other reactive or refractory elements may be added to the melt. Commercial compositions contain

---

\* Numerical notations refer to literature listed under references.

6-12 intentionally added elements and have 4-6 phases in their microstructure. The two major phases in the microstructure are a face-centered cubic phase called gamma which is the matrix phase and a dispersed ordered face-centered cubic phase called gamma prime. Small amounts of carbides, borides and other intermetallic compounds are frequently present.

Although the physical phenomena which contribute to the excellent elevated temperature strength of these alloys are not understood, there is general agreement among superalloy metallurgists that interaction between the gamma and gamma prime phases must somehow account for the unique properties of this system. It is also generally accepted that addition of the refractory metals to the nickel-base superalloys can significantly influence their high temperature properties.

The development of the superalloys has been accompanied by abundant literature relating to the formulation of commercial compositions, their heat treatments, fabrication, physical metallurgy, and uses. Because of the complicated nature of the commercial compositions previously cited, it is difficult to isolate effects of individual elements and phases on the properties of the alloys. The first analytical approach toward this end was offered in 1964.<sup>2</sup>

This study was initiated to obtain information on the manner in which some of the more important alloying elements are partitioned between the gamma and the gamma prime phases. The elements selected for study were aluminum, chromium, titanium, molybdenum and tungsten.

Carbon and boron were specifically held to levels low enough to preclude the formation of carbides and borides. The resulting alloys would then resemble commercial alloys except as just noted, but would lend themselves to simple phase separation procedures and phase analysis.

The objective of this study is to develop a system of mathematical expressions which describe the phase boundaries of the gamma and gamma prime regions of the nickel-chromium-aluminum-titanium-molybdenum-tungsten system at 850° C and the partitioning of the elements between the two phases. This information should permit better estimation of how alloying will change the relative amount of the phases, and when correlated with X-ray data may permit estimation of the lattice mismatch between the two phases. The lattice mismatch is believed by some investigators to be of great importance to the mechanical properties of these alloys. Although no mechanical properties will be determined in this study, it is hoped that the eventual use of this information will result in an improved understanding of the nickel-base superalloys and the development of improved alloys.

## II BACKGROUND

### Phase Diagrams

Published diagrams. - The most advanced phase diagrams available, pertaining to Ni-base superalloys, are the 1000° and 750° C isotherms of the Ni-Cr-Ti-Al system in reference 3. The Ni-rich quaternary section shown in Figure 1(a) provides a perspective on the relationship between the  $\gamma$  and  $\gamma'$  phase fields, but because the diagram is a two-dimensional representation of a three dimensional figure it is difficult to use for specific analysis. The pseudo-ternary diagram shown by Taylor in reference 3 and reproduced here as Figure 1(b) is of greater engineering value because of the ease with which it can be used. This diagram, which is shown for a constant nickel concentration of 75%,\* indicates that at 750° C  $\gamma'$  can dissolve 6% Cr\* when no Ti is present. At the Ti solubility limit of 15% in  $\gamma'$  only about 2% Cr can be retained in the  $\gamma'$ . This diagram also shows that the  $\gamma$  has a maximum solubility for Ti of 4% and for Al of 5%. The addition of Ti to Ti-free  $\gamma$  initially drastically reduces the solubility of Ti in the  $\gamma$ .

The recent work of Loomis<sup>4</sup> studied the effect of Mo additions to Ni-14% Cr alloys at several Al concentrations. His work included a limited study of Ti. He showed that additions of Mo reduce the

---

\*Concentrations will be in atomic percent unless otherwise noted.

solubility of Cr in the  $\gamma'$  and suggested that Mo substitutes for Cr in the  $\gamma'$  phase. Additions of Mo increased the  $\gamma'$  solution temperature and at a constant temperature increase the amount of  $\gamma'$ . The addition of Ti substantially reduces the solubility of Mo, Cr, and Al in  $\gamma'$ .

Havalda<sup>5</sup> showed that for alloys of Ni- 20% Cr at 850° C that Ti additions reduce the solubility of Al in  $\gamma$  and that W additions also reduce the solubility of Al in  $\gamma$ . These alloys had a carbon addition of 0.15 weight %.

The Ni-Al-W diagram at 800° C is shown in reference 6. The solubility of Al in both  $\gamma$  and  $\gamma'$  is increased with increasing W additions. The  $\gamma$  solvus curve at 900° C for the Ni-Al-Mo system is shown in reference 7. Molybdenum additions decrease the solubility of Al in the  $\gamma$ .

The three ternary systems which bound the quaternary in reference 3 are shown in reference 3 and the details of their development are discussed in references 8 to 11. The Ni-Cr-Al<sup>8</sup> diagram shown in Figure 2 is useful in understanding the behavior of the superalloys. Chromium additions reduce the Al in the  $\gamma$  from 12% at 0% Cr to a minimum of 7% Al at approximately 20% Cr. Chromium additions to the  $\gamma'$  phase initially reduce the Al solubility of the  $\gamma'$  in equilibrium with  $\gamma$  from 23% to a minimum of 12% at approximately 15% Cr. The tie lines show that the Cr concentration in the  $\gamma$  is approximately three times the Cr concentration in the  $\gamma'$ . The  $\gamma - (\gamma + \gamma')$  boundary location was confirmed in reference 9.

The Ni-Ti-Al diagram<sup>10</sup> at 750° C is shown in Figure 3. As was previously mentioned, it can be seen that small additions of Ti to Ti-free  $\gamma$  reduce the solubility of Al in the  $\gamma$ . The diagram also shows that  $\gamma'$  can dissolve approximately 15% Ti, apparently substituting for Al. At the  $\gamma'$  solvus, the total of the Al plus the Ti in the  $\gamma'$  remains nearly constant at 22% as Ti is added to the  $\gamma'$ .

Although several ternary systems relevant to the Ni-Cr-Al-Ti-Mo-W system have been published they add little to the understanding of the superalloys if they do not include Al because the  $\gamma'$  phase requires Al to stabilize it. Systems which do not contain Al are therefore not discussed.

Phase chemistry. - In the past several years there have been several investigations which did not produce phase diagrams in the classical sense, but did determine the chemical composition of the  $\gamma'$  or  $\gamma$  phase in nickel-base superalloys. The analyses were usually conducted on commercial compositions containing 3-5 phases.

The most extensive investigation of this type is that of Krieger and Baris.<sup>12</sup> An investigation was conducted on 15 commercial alloys which were generally in heat treated conditions typical of the alloys as placed in service. Their results are summarized in Table 1. Table 1(a) summarizes the amount of  $\gamma'$  in the alloys, Table 1(b) summarizes the composition of the  $\gamma$  phases and Table 1(c) summarizes the composition of the  $\gamma'$  phases studied by Krieger and Baris. Their analyses show that  $\gamma'$  coexisting with  $\gamma$  will contain only up to 4.1% Cr and 2.3% Mo. The  $\gamma$  solubility

for Ti is 1.5% and for Al is 8.1%. Chromium and molybdenum partition primarily to the  $\gamma$ , while aluminum and titanium partition mostly to the  $\gamma'$ . Tungsten appears to partition nearly equally between the two phases.

Mihalison and Pasquine<sup>13</sup> described phase chemistry results obtained in three superalloys. Their results are in good agreement with the results in reference 12. Results reported in the Soviet Union<sup>14</sup> for  $\gamma'$  in two Soviet superalloys are also similar to those mentioned above.

Phase chemistry estimation. - To help understand and control the precipitation of undesirable phases, the metallurgists studying superalloys developed several procedures for estimating the composition of the  $\gamma$  phase. The first of these was described in reference 2. In this method, the  $\gamma'$  elements are subtracted from the alloy composition using the assumption that all the Al and Ti form  $\gamma'$  of a composition represented by  $Ni_3(Al,Ti)$ . A similar method was proposed by Woodyatt et al.,<sup>15</sup> but a slightly different  $\gamma'$  composition was proposed and the Cr composition of the  $\gamma'$  was related to the melt Cr concentration. Reference 15 also attempted to account for the formation of borides and carbides in the method. Like reference 1 the method assumed that all Al and Ti (as well as some other elements) partitioned to the  $\gamma'$ . A profusion of this type of calculation resulted as exemplified by reference 16 where 12 such calculations are shown. All of these assumed that no Al or Ti would be present in the  $\gamma$  and used relatively fixed

compositions for the  $\gamma'$ .

In an effort to avoid the apparent problems associated with the uncertainties of the  $\gamma'$  composition and to allow the presence of Al to be shown in the  $\gamma$  phase, a method using a geometric solution of the phase diagram from reference 8 (Ni-Al-Cr) was developed.<sup>17</sup> This geometric analysis was soon extended to account for the influence of Ti on the Al concentration in the  $\gamma$ .<sup>18</sup> The calculation procedure proposed in reference 18 was based on a geometric solution of Taylor's quaternary (Ni-Al-Cr-Ti) shown in reference 3. The method in reference 18 has the ability to estimate the compositions reported by Krieger and Baris<sup>12</sup> and Mihalisin and Pasquine.<sup>13</sup> Although, in principle, the method proposed in reference 18 could be used to estimate the  $\gamma'$  chemistry, the author made no effort to do so.

Decker<sup>19</sup> proposed a calculation which could estimate the composition of both the  $\gamma$  and  $\gamma'$  phases. Decker's calculation uses regression analyses to account for the carbide phases and the amount of  $\gamma'$  in the alloy. This calculation then uses a mass balance technique to calculate the phase composition from the melt analysis, although no actual phase chemical analyses are listed. It is assumed they would agree with the data of Krieger and Baris<sup>12</sup> and Mihalisin and Pasquine<sup>13</sup> because these data were used as the basis for the calculation.

#### Lattice Mismatch

The importance of the lattice mismatch between  $\gamma$  and  $\gamma'$  is generally agreed upon by the various investigators. Initial

interest was concerned with the relation between the lattice mismatch and the  $\gamma'$  morphology.<sup>20</sup> Recently the relation between the mismatch and the mechanical behavior of the alloys has been studied. Davies and Johnston<sup>21</sup> have indicated that to achieve optimum creep resistance an alloy should contain a fine dispersion of approximately 60 volume percent  $\gamma'$ . To maximize the stability of the  $\gamma'$  dispersion at high temperature, zero mismatch should exist between the two phases.

Decker and Mihalisin<sup>22</sup> have concluded that coherency strains make a potent contribution to the age hardening strength of these alloys under conditions of non-diffusional creep at temperatures below 0.6 of the melting point. Their experiment was designed such that the mismatch would be the parameter altered to the greatest degree. They did this by adding approximately 2% each, Cb, Ta, V, Si, Mn, Ga, and C to alloys of Ni-14% Al. They assumed that the amount of  $\gamma'$  remained constant and the solution hardening could be accounted for in their experiment.

Maniar et al.<sup>23</sup> studied the effect of mismatch on mechanical behavior of Ni and Fe/Ni-base alloys. The alloys studied showed a sharp maximum at a mismatch of 0.07% in stress rupture life for the Ni-base superalloys. No correlation was observed with a Fe/Ni-base superalloy. When Mo was added to the Ni-base alloys, the mismatch decreased and the rupture life increased. Chromium additions decreased the mismatch, but the effect on life was not great. It should be noted that no evidence exists that the volume fraction of

$\gamma'$  or the size of the  $\gamma'$  particles was constant or controlled in the experiments.

Loomis<sup>4</sup> was able to show a linear correlation between the lattice parameters of both  $\gamma$  and  $\gamma'$  and the composition of the phases. His study included Al, Cr, Mo, and Ti. Cr has the least effect on the lattice parameter while adding Ti expands the lattice three times faster and adding Mo expands the lattice 4 times faster than Cr. The most striking point of this was that the same atomic coefficients could be used to describe the behavior of adding alloy elements to both phases. This fact results in the expectation that the result of adding alloy elements to a superalloy on its lattice mismatch will be as much effected by how the alloy partitions between the two phases as by its intrinsic effect on the lattice parameter of each phase.

Havalda<sup>5</sup> has shown that W additions to alloys containing 20% Cr reduce the lattice mismatch between  $\gamma$  and  $\gamma'$ . Zero mismatch is achieved near 8% W. Taylor and Floyd<sup>8</sup> showed that in Ni-Cr-Al ternary alloys having 75% Ni and 70% Ni the lattice parameter of both phases decreases as Al is replaced by Cr. At 70% Ni, zero mismatch occurs at approximately 20% Cr, 10% Al. At 75% Ni, zero mismatch occurs at approximately 10% Cr, 15% Al.

When considering all of the above investigations, one should bear in mind that it is experimentally very difficult to measure the mismatch between the two phases directly because of the fact that the mismatch tends to be below 1% and only 10 to 20 volume

percent of  $\gamma'$  frequently is present in the alloy. Some investigators therefore find it expedient to measure the  $\gamma$  parameters in situ, but measure the  $\gamma'$  parameters in extracted residues. The lattice parameter of the extracted materials will (except where the in situ mismatch is zero) change as a result of removing the constraint of the other phase. The results of one investigation may therefore not be directly comparable to another. One would expect that the trends observed should be consistent and it is presumed that an optimum lattice mismatch exists for various service conditions. If the metallurgist is to exercise control on the mismatch, knowledge of how various elements affect the lattice parameter of the phases and of how the elements are partitioned between the phases is required.

#### Ordering in Gamma Prime

One model proposed to account for the unusual elevated strength properties of the Ni-base superalloys<sup>24</sup> relates the strength to the antiphase boundary energy in the  $\gamma'$ . The antiphase boundary energy is related to the degree of long range order (S) of the phase.

Unfortunately little information is available concerning the ordering of  $\gamma'$  and the broad use of approaches similar to reference 24 has been restricted. Gamma prime in pure form ( $\text{Ni}_3\text{Al}$ ) is an ordered face-centered cubic structure of the  $\text{Cu}_3\text{Al}$  ( $\text{LI}_2$ ) type. It has been reported to have an order parameter (S) of 0.99 at room temperature.<sup>25</sup>

Dorfeld and Phillips<sup>25</sup> also measured the order parameter (S) of

the phase  $\gamma'$  in a commercial alloy René 63. The alloy had been given a multistep heat treatment, the last step of which was holding at 760° C for 16 hours. S measured at room temperature was 0.78.

In contrast, Mihalisin<sup>26</sup> has reported S for  $\gamma'$  in several commercial alloys to vary from 0.82 to 0.96. In considering IN 731, IN 713 C and IN 713 LC, it was found IN 731 had the lowest S with a value of approximately 0.83. Alloy IN 713 C had an S of 0.90 and alloy IN 713 LC had an S of approximately 0.95. He was unable to correlate prior thermal and mechanical history with variations in S observed at room temperature.

In both of the above studies some Cr, Mo, and Co were assumed to reside on Ni sites (face centers) in the fully ordered state. The authors assumed that for perfect order a formula like  $(\text{Ni}_{.81}, \text{Co}_{.12}, \text{Cr}_{.07})_3(\text{Al}_{.6}, \text{Ti}_{.28}, \text{Cr}_{.12})$  which was used in reference 25 can describe the alloyed  $\gamma'$ . For some compositions Mo also appears in both the parentheses.

For alloys IN 713 C and IN 713 LC,<sup>26</sup> however, Ni accounted for 97-98% of the Ni site occupancy. In the other two alloys Ni plus Co accounted for over 90% of the Ni site occupancy in the fully ordered state.

These papers also show one of the difficulties that metallurgists encounter; that is, deciding if an observed phase is  $\gamma$  or  $\gamma'$ . As previously noted, both are face-centered cubic and have essentially the same lattice parameter. In pure  $\text{Ni}_3\text{Al}$ , the intensity of the

(100) reflection is approximately 20% of the (200) in the highest state of order.<sup>26</sup> This intensity ratio decreases with alloying and decrease in S. The ratio was 4% in René 63 and 7-10% in the alloys studied by Mihalisin. It may well be that with further alloying or decrease in S that the intensity of the (100) might become too weak to be readily observed. The (200) is the second most intense line of the fundamental lines and the (100) is the most intense of the superlattice lines. The use of superlattice lines to positively identify  $\gamma'$  relative to  $\gamma$  can be seen to be hazardous. The presence of the superlattice lines is positive identification for  $\gamma'$ , but their absence should not exclude the identification of  $\gamma'$  in highly alloyed materials.

#### Occurrence of Other Phases

After the identification of sigma phase in a nickel-base superalloy,<sup>27</sup> considerable effort has been directed toward understanding the relationship between the occurrence of sigma and similar phases and mechanical properties. In 1968, a 3-day conference was held on the subject.<sup>28</sup> Papers presented at that conference and many subsequent ones,<sup>16,29-33</sup> have shown that precipitation of sigma and mu phases may occur in nickel-base superalloys and in some materials large decreases in ductility and stress rupture life have been correlated with the precipitation of these phases.

Beattie and Hagel<sup>34</sup> surveyed the superalloy systems for the occurrence of phases using a statistically designed experiment. A quasi-ternary system of Fe-Ni-Co was studied by alloying with W, Ti,

Si, Cr, Cb, and C. After aging 1000 hours at 815° C, 15 phases were identified. Phases other than  $\gamma$ ,  $\gamma'$  carbides and nitrides which were found are eta, epsilon, laves, sigma, mu, chi, beta and G. One of the authors' more interesting findings was that of 60 new compositions melted in a complex system, no previously unknown phases were identified. The structures of the precipitating phases were found to be no more complex than the structures found in ternary systems. No structures that require four different atomic species were found. The authors also noticed that alloying appeared to reduce the number of possible structures by eliminating some of the more complex ones in favor of simple structural types.

The occurrence of sigma phase in Ni-base alloys at intermediate temperatures was recently studied by Kirby.<sup>35</sup> The  $\gamma$  plus sigma phase boundary was determined in a series of aluminum free alloys and Mo and W were found to be equal in their sigma promoting characteristics. The investigation further demonstrated that a "sigma free" composition could be made to precipitate sigma by diffusing in sufficient Al to cause the precipitation of  $\gamma'$ . Thus the phase computation philosophy set forth by Boesch and Slaney<sup>3</sup> and by many others subsequently has been demonstrated by a simple experiment.

#### Summary Remarks

It should be apparent from the preceding sections that the structure and resulting mechanical properties of Ni-base superalloys are associated with the occurrence and composition of several phases.

If it could be predicted which phases occur as a result of alloy additions and the chemical composition of these phases could be established, new and better alloys could be developed. The information required is obtained from phase diagrams, but phase diagrams in the classical sense cannot exist for a 6 component system because no graphical representation is possible. This investigator<sup>16,17</sup> has previously shown that the information which is normally available in 3 and 4 component phase diagrams can be treated mathematically to assist in determining the composition of conjugate phases in a two phase field given the composition of the two phase alloy. Ivanov<sup>36</sup> has treated a multi-component phase diagram algebraically to allow useful information to be obtained.

The object of this investigation is to determine the "phase diagram" for the Ni-rich region of the Ni-Al-Cr-Ti-Mo-W system. The diagram will be restricted to the 850° C isotherm and will only describe the  $\gamma - \gamma'$  two phase field. The "phase diagram" will be a series of mathematical expressions which can be examined with the use of a digital computer to yield composition information of conjugate phases.

### III EXPERIMENTAL PROCEDURES

The method of determining the effect of alloying on the  $\gamma - \gamma'$  relationships in nickel-base superalloys was to prepare a series of two phase alloys containing Ni, Cr, Al, Ti, Mo and W in concentrations representative of commercial superalloys. The  $\gamma'$  was quantitatively extracted from the alloy and chemically analyzed. Alloy samples and extracted  $\gamma'$  were examined by X-ray diffraction, light and scanning electron microscopy and electron microprobe analysis. The various methods used are described below.

#### Selection and Preparation of Alloys

Two preliminary alloys were selected to determine whether the procedures intended to be used could be applied to the alloy system to be studied. These alloys are designated as alloys 98 and 99 in Table 2. These alloys were prepared by the methods to be described later and no unusual behavior was noted.

Thirty six compositions were then selected which would represent commercial alloy composition ranges. The alloy compositions are designated as alloys 1-36 in Table 2 and the maximum, minimum and intermediate levels melted for each element are shown in Table 3. The initial design is a fraction of a 3 level factorial design. The specific experimental design was taken from the first four

blocks of plan 3.5.9 of reference 37. A fractional factorial design was used to insure that all regions of the experimental space would be uniformly covered.

Thirteen additional compositions were later added to the design when it was observed that approximately one-third of the original compositions were not two phase alloys. The additional heats were selected by using the same experimental design, but changing the composition limits as shown in Table 3. Only those compositions were prepared which were not two phase in alloys 1-36 and which could reasonably be expected to be two phase based on a phase stability calculation previously used by the author.<sup>38</sup> These compositions are designated as 37-49 in Table 2.

All alloys were prepared from high purity virgin metals. The form and composition of the raw materials are shown in Table 4. The charge weights varied from 1300 to 1800 grams. Stabilized zirconia crucibles were used for melting, a new crucible being used for each melt.

The alloys were vacuum induction melted and investment cast. The initial charge consisted of Ni, Ti and Mo and/or W. The furnace was evacuated to less than 10 microns before heating was initiated. After the initial charge plus any additional Ni which would not fit in the crucible had been melted, the furnace was backfilled with argon to approximately 1/3 atmosphere. Chromium was then added to the melt and the system was pumped down to 10-20 microns. After clearing the dross which formed when the Cr was added, the system

was backfilled with argon to approximately 1/2 atmosphere. Aluminum was added to the melt and it was then brought to the pouring temperature. All melts were poured at approximately 1650° C. The investment molds were made of zircon and were preheated and held at 812° C in a separate mold heating furnace located in the vacuum chamber. After pouring, the castings were allowed to cool at least 20 minutes before being removed from the vacuum chamber.

A casting consisted of six bars 1-1/4 cm diameter and 7-1/2 cm long. A casting with the gates and risers still attached is shown in Figure 4. The bars were cut from the casting with an abrasive cut-off wheel and sandblasted prior to heat treatment.

#### Heat Treatment

One bar from each heat was heat treated. The heat treatments were conducted in an argon atmosphere to keep surface oxidation to a low level. The alloys were heated to 1190° C for 4 hours and air cooled to room temperature. This treatment was intended to reduce segregation effects and dissolve a large fraction of  $\gamma'$  in the alloys. The alloys were then heated to 850° C and held 1008 hours prior to being air cooled to room temperature. The bars were heat treated (1008 hr treatment) in three batches. The same furnace was used for each batch and the same control settings were used on the furnace. The temperature was monitored daily and the deviation was  $\pm 2^\circ$  C.

### Location of Test Specimens

Immediately following heat treatment, the bars were ground to remove at least 0.02 mm from the surface. This was to remove any regions having alloy depletion or internal oxidation. The bars were cut to provide cylinders approximately 1 cm long. Three cylinders were cut from each sample. The end one (exposed end oxidized) was used for metallography. The center cylinder was used for extractions and the third was submitted for chemical analysis. A sketch of the bar and specimen layout is shown in Figure 5. This procedure was used to reduce the influence of macroscopic segregation in the longitudinal direction of the cast cylinder.

### Metallography

Specimens were examined using both light and scanning electron microscopes. The same specimen preparation was used for both types of microscopy. The specimens were mounted in bakelite so as to allow examination of the unoxidized surface. The mount was ground using abrasive papers through 600 grit. Intermediate and final polishings were accomplished using 0.3 and 0.6 micron alumina on Microcloth.\*

All alloys were examined in three conditions with the light microscope. The samples were first examined unetched. The body-centered cubic (Cr, Mo, W) phases were usually easily distinguished in this condition. The second examination used an etch of 1% KOH.

---

\*Registered trademark of Adolph Buehler Company.

The etch was electrolytic using 6-8 volts for approximately 5 seconds. The KOH etch revealed the presence of sigma and mu phases in addition to the body-centered cubic phases without distinguishing between  $\gamma$  and  $\gamma'$ . The KOH etch was removed using the last two polishing steps then an etch of 33 parts  $H_2O$ , 33 parts  $HNO_3$ , 33 parts  $CH_3COOH$ , 1 part HF (mixed acids) was applied by swabbing or immersion. This etch revealed the features described above and the  $\gamma - \gamma'$  structure of the alloys. This etch was also used for scanning electron microscopy.

#### Extraction of Phases

Prior to extraction, the flat surfaces of the specimens were ground through 180 grit abrasive paper. A length of chromel wire was welded to the specimen and the arc strike was removed by hand grinding. Heat shrinkable plastic tubing was placed over the wire to act as an electric insulator and to protect it from corrosion. The specimens were ultrasonically washed in acetone and dried. Each specimen was weighed prior to the extraction process.

The first extraction process used on each alloy was 10% HCl in methanol. One percent tartaric acid was added to the electrolyte when W was present in the alloy. Extractions were conducted with the sample as the anode and Pt mesh as the cathode for 4 to 6 hours with the current density of approximately  $0.1 \text{ a/cm}^2$ . Evaporation losses were made up by periodic additions of full strength electrolyte. Any residue adhering to the specimen was removed by scraping with a spatula. Then, the specimen was ultrasonically cleaned in

methanol, dried and weighed. All residues were collected on a pre-weighed 0.5 micron Solvinert\* filter. The residues were washed with water, then methanol, dried and weighed. The fraction of residue was calculated as the weight of recovered residue divided by the loss in weight of the sample.

In the Ni-base-superalloys, the HCl-methanol extraction procedure is expected to dissolve  $\gamma$  and  $\gamma'$ . The electrolyte is not expected to dissolve sigma, mu, laves, most carbides, nitrides.<sup>16</sup> If the residue of this extraction were low enough (less than 0.5%) to suggest that the alloy could be assumed to be essentially two phase an electrolytic extraction procedure was then used to separate the  $\gamma'$  from  $\gamma$ .

To separate  $\gamma'$  from  $\gamma$  an electrolyte of 2% ammonium sulfate and 2% citric acid in water was used. This electrolyte has been reported to separate quantitatively the  $\gamma'$  over a wide range of commercial alloy compositions.<sup>12</sup> The electrolysis was conducted for 2 to 6 hours at 0.02 a/cm<sup>2</sup>. The specimens were weighed before the extraction was conducted. At the end of the process, the specimens were washed by allowing them to soak in clean water for at least 15 minutes. Three such washes were used prior to drying and weighing. All loose residues were collected on Solvinert\* filters as described for the HCl procedure. The dried metallic sample was weighed and the adherent residue was removed by scraping with a spatula and scalpel. The specimen was then wire brushed and ultrasonically

---

\*Registered trademark of Millipore Corp.

cleaned in methanol. The dried clean sample was given a final weighing. The fraction of  $\gamma'$  is taken as the weight loss between the second and third weighings plus the weight of the solids on the filter; divided by the total weight loss of the sample. This procedure was used in duplicate on most alloys. Where the between run agreement was poor, a third run was made.

In some cases, where the Cr and Al of the sample was low, the sample was passive under the conditions described for the ammonium sulfate electrolyte. In these instances, a similar procedure was used with a 10% phosphoric acid electrolyte. It is likely that this procedure is not quantitative for  $\gamma'$ ,<sup>12</sup> but the residue collected is believed to represent the chemical composition of the  $\gamma'$  accurately.<sup>4</sup> The  $\gamma'$  residues and selected HCl residues were submitted for chemical analysis. All residues were examined by X-ray diffraction.

#### Chemical Analysis

The weight of the residues resulting from the above extraction procedures was usually less than 0.3 gms. Analysis of up to five elements was required for the program. It is apparent that to analyze a large amount of such small samples that an instrument approach was required. The investigator selected a recently developed analysis system<sup>39</sup> which uses arc emission spectroscopy that is capable of suitable accuracy with as little as 10 micrograms of sample. All chemical analysis used in this investigation, except as will be discussed below, were obtained by the analysis system

described in reference 39. The analyses were provided by NASA Lewis Research Center.

The lowest levels of Ti examined in the investigation were below the capability of the analysis system. These determinations were made by using densitometer measurements on plates made from the same samples used for the other analyses.

To obtain a check on the suitability of the analysis system to be used, 11 arbitrarily selected alloy samples were submitted to a separate and independent chemical laboratory. The results of these analyses and those of the method to be used in this investigation are compared with the aim (melting charge) in Table 5. Both of the analyzed compositions are in good agreement with the aim composition and with each other. The chemical analyses of all the heats are compared to the aim in Table 2.

#### X-ray Diffraction

Identification of phases. - The identification of phases is based on X-ray diffraction patterns obtained from extracted residues. The extracted residues were sprinkled on glass microscope slides with a micro-spatula. The residues were then bonded to the slide with 10% collodion in amyl acetate. The diffraction patterns were made using a GE XRD-3 diffractometer. Both Ni-filtered Cu and V-filtered Cr radiations were used. The patterns scanned from  $20^\circ 2\theta$  to approximately  $140^\circ 2\theta$ . The patterns were compared with published patterns,<sup>33,40</sup> unpublished data from Task Group 001, Committee E-4 on Metallography of ASTM and computer synthesized patterns. As a

check, most patterns were indexed and a refined lattice parameter was calculated using a computer program; HERTA4.<sup>41</sup> The ability to calculate a refined lattice parameter having a low standard deviation is considered by the investigator as indication that the correct structure and indexing was used; therefore the identification (of structure type) is accepted. The phases identified in each heat is summarized in Table 6.

Lattice parameters. - The lattice parameters of the  $\gamma'$  samples were determined from samples prepared in the manner described above. Direct measurement of the lattice parameter of the  $\gamma$  phase was not possible because of the large grain size in the castings. In most cases only one or two reflections could be found on cast specimens. To allow determination of the  $\gamma$  phase lattice parameter, filings were obtained from the cast and heat treated samples. The filings were vacuum encapsulated in quartz and the capsules were then heated at 815° C for 30 minutes to allow recovery to occur. Because the temperature was below the long time aging temperature and the time was short, it was thought that this data could adequately represent cast and aged material. The filings were removed from the capsules and placed on glass slides in the manner previously discussed.

Diffraction patterns were made using Ni-filtered Cu radiation, and a scanning speed of 2° 2 $\theta$  per minute. The receiving slit was 0.1° 2 $\theta$ . The diffractometer charts were read to 0.1° 2 $\theta$  and the HERTA4 computer program was used to refine the lattice param-

eters. The extrapolation function used was the  $\cos \theta \cot \theta$  function which is suggested by Vogel and Kempter<sup>41</sup> as being the most appropriate for diffractometer data. The lattice parameters of  $\gamma$  and  $\gamma'$  are listed in Table 7.

Relative intensities. - The intensity data used for estimating the long range order parameter (S) was obtained from the  $\gamma'$  specimens described above. To eliminate errors that may arise from preferred orientations formed during specimen preparation, the intensity of the (100) and (200) reflections were measured. Vanadium-filtered Cr radiation was used. The scanning speed was  $0.2^\circ$  2 $\theta$  per minute and a  $3^\circ$  receiving slit was used. The (100) line was scanned from  $34^\circ$  to approximately  $40^\circ$ , the (200) line was scanned from  $78^\circ$  to approximately  $83^\circ$ . The intensities used were the peak height corrected for average background.

The intensity calculations for "ideal" ordering were made using a computer program POWD2.<sup>42</sup> This calculation is capable of synthesizing diffractometer patterns using a Cauchy distribution function or a Gaussian distribution function for the peak profile. For this study the Cauchy form was selected. The measured peak heights were compared to the calculated peak heights to obtain relative intensities.

This same computer program<sup>42</sup> was also used to prepare patterns against which unknown patterns were compared as previously discussed under Identification of Phases. In the process of calculating the X-ray diffraction pattern, the density of the material is calculated

and is part of the output. These values were used for the X-ray density values of  $\gamma'$ .

#### Other Measurements

Density measurements. - The density of those alloys which could be calculated from X-ray diffraction data and chemical analysis were measured. Archimedes method of weighing the material dry and in water was used. The density is the dry weight divided by the difference between the wet and dry weight.

Gamma prime volume. - To obtain an independent check on the amount of  $\gamma'$  in the alloys, the volume fraction was measured by the use of point counting on scanning electron micrographs taken from selected samples. A grid having 153 intersections was overlaid on the micrograph and the number of intersections lying in  $\gamma'$  were counted. The fraction of such points is taken as the volume fraction of  $\gamma'$ .<sup>43</sup>

#### IV RESULTS AND DISCUSSION

The 51 alloys shown in Table 2 were melted and analyzed using light microscopy and X-ray diffraction of electrolytically extracted residues. The alloys could then be separated into three groups. The first group was single phase alloys and included only alloys 1 and 11; the second group contained more than two phases. The 22 alloys listed in Table VI formed the multiphase alloy group. The third group contained those alloys which could be assumed to contain only  $\gamma$  and  $\gamma'$ . Specifically these were alloys which produced less than 0.5% residue in the HCl electrolytic extraction and that residue could not be identified as a body-centered cubic phase such as Cr, Mo or W, a carbide, nitride, sigma, mu or similar phase. It is assumed that the residues were oxides, but they were not positively identified as such. Furthermore, these minor phases were not acicular and could not be identified using light microscopy.

This third group of alloys contained 27 compositions. The alloys are listed in Table 8. The amount of  $\gamma'$  and unidentified material which was extracted are shown in Table 8. It was this third group of alloys which was most extensively studied.

##### Gamma Prime Composition

The average compositions of the residues obtained using the ammonium sulfate or phosphoric acid electrolytes on the third group

of alloys are shown in Table 9. Alloy 21 is not included because it was not possible to obtain a sufficient quantity of residue to analyze. The analysis shown were conducted by the emission spectroscopy procedure previously discussed. Each element was analyzed; then it was normalized to provide a sum of the elements of 100%. The chemical analysis procedure used automatically rejected any results where the sum of detected elements differed from 100% by more than 6%. This form of normalization was used so as to avoid biasing any single element with experimental error. A summation to 100% is required to allow a mass balance determination of the  $\gamma$  composition.

The Ni content of the  $\gamma'$  is nearly constant and varies only from 72.1% to 78%. The Al ranges from 7.8% to 17.5%; the Cr varies from 1.5% to 8.9% and the Ti varies from 0.3% to 13.9%. Where Mo was intentionally added, (non-zero) Mo content varies from 1.1% to 3.9% and where W was intentionally added, (non-zero) W varies from 1.7% to 7.2%. The sample standard deviation (s) for each element except Ni is shown in Table 9 and is less than 1/3 the range of each element observed. This suggests that the spread in observed compositions is significant when compared to analytical errors.

The concentrations of Al, Cr, Mo, Ti, and W observed in this study compare well with those observed by Kriege and Baris<sup>12</sup> shown in Table 1(c), the observations of Loomis<sup>4</sup> and Mihalisin and Pasquine.<sup>13</sup> The major difference lies in the fact that Ni

concentrations in this investigation were found to exceed 75% more frequently than in those cited in reference 12. It is not clear whether this difference is real and perhaps a result of the lower carbon and boron levels used in this investigation or that the difference lies in the chemical analysis procedures used. The normalization of the analyses to 100% is not believed to be the cause of Ni exceeding 75% because in many instances the total composition was less than 100% when the Ni exceeded 75%. If Ni were determined by difference (as was the case in the cited references) the Ni concentrations reported here would in fact be greater in magnitude.

In this study it appears that  $\gamma'$  which is conjugate with  $\gamma$  has an approximate formula  $Ni_3(X)$  where X may be Al, Cr, Mo, Ti or W. On the basis of the chemical analyses, the phase appears to have an equal probability of having deficient or excess Ni compared to 75% Ni. Fifteen of 26 compositions have more than 75% Ni in the  $\gamma'$ . The range of Ni in the  $\gamma'$  in this investigation is almost identical to that observed in reference 4, but in reference 4 most of the compositions exceeded 75% Ni. It appears that the Ni can be assumed to remain nearly constant at 75% while the other elements substitute for each other acting as Al would in the ideal binary compound  $Ni_3Al$ .

#### Amount of Gamma Prime

The amount of  $\gamma'$  electrolytically extracted from the alloys is shown in Table 8. The amounts recovered using the ammonium sulfate

base electrolyte varied from less than 1 weight % to greater than 55%.

To check on the quantitative nature of this electrolyte, several compositions were examined using scanning electron microscopy and point counting of the micrographs to estimate the volume fraction of  $\gamma'$ . Where sufficient data was available, the measured weight fraction was converted to volume fraction using the X-ray densities of the phases (calculated volume %). The observed and calculated volume fractions are compared in Table 10. The agreement is considered good, particularly when one takes into account that the volume fractions were measured at 5000 and 10000 X magnifications, where the volume observed is very small compared to that dissolved in the extraction process.

The above procedure provided a fairly direct method of verification of the weight fraction determination. However insight into the nature of the extraction process can also be obtained by comparing the density of the castings with the density calculated using the X-ray density of each phase and the measured weight fraction. These data are shown in Table 11. The agreement between the measured and calculated densities is good. It should be noted particularly that there is no bias toward either greater or smaller observed densities compared to measured densities. If the extraction method was not quantitative and no extraneous phases were precipitated, then one would expect that the calculated density would tend to be biased toward the density of the  $\gamma$ . This occurs because the  $\gamma$  phase

would appear to be present in a greater amount than is truly present. Because this type of bias was not observed and because the measured and observed volume fractions were in good agreement the ammonium sulfate extraction procedure is assumed to be quantitative for the  $\gamma'$  phase provided that no sigma, mu, or body-centered-cubic phases were identified in the alloys.

It is generally believed that the amount of  $\gamma'$  is strongly related to the amount of Al and Ti in the alloys. This thesis, in fact is an important part of the "phase calculations" in references 2, 15 and 16. These calculations assume that the amount of  $\gamma'$  can be determined by assuming that all of the Al and Ti, together with some other elements, partition to the  $\gamma'$ . Decker<sup>19</sup> uses an equation relating the volume fraction of  $\gamma'$  to the composition of the melt to estimate the amount of the phase. His equation was arrived at by using regression analysis on the data for some commercial alloys in references 12 and 13. His equation<sup>44</sup>

$$\text{Vol } \% \gamma' = .333 \times \text{Ni} + 2.6878 \times \text{Ti} + 3.5686 \times \text{W} + 13.1143 \times \text{Ta} \\ + 2.9538 \times \text{Al} - 1.5728 \times \text{Fe} + 5.9347 \times \text{V} - 12.7657$$

where Ni, Ti, etc. are atomic % of melt, can be seen to indicate that several other elements in addition to Al and Ti strongly influence the amount of  $\gamma'$  in the alloy. When this equation was applied to the alloys melted in this work it was found that the estimated fractions of  $\gamma'$  failed to agree with the experimental observations.

Several 1<sup>st</sup> to 3<sup>rd</sup> degree equations were used as models for

regression equations for the data obtained in this study. The models were examined using two computer programs. One, NEWRAP<sup>45</sup> is a multiple linear regression analysis which provides internal remodeling of the equation. The second, CRSPLT,<sup>45</sup> is primarily a plotting routine which simply crossplots all variables. In addition to the plots, a correlation matrix is provided by the program. No strong correlation with first degree terms (such as those used by Decker) was apparent. It was possible to develop models, using 20 terms, where some terms were of the 2<sup>nd</sup> degree with correlation coefficients in excess of 0.9. If, however, the duplicated measurements were used to provide an independent measure of error, the regressions suffered from lack of fit and their use beyond the data which produced them would be extremely hazardous. These equations were found to be of little value in predicting the fraction of  $\gamma'$  in the alloys studied in reference 12.

Perhaps a better perspective on this problem can be obtained by referring to Figure 2, the 750° C section of the Ni-Cr-Al phase diagram. For 2 phase ( $\gamma + \gamma'$ ) alloys containing less than 15% Cr, increasing Al in the alloys will increase the  $\gamma'$  fraction. If the Cr is greater than 15%, the problem is more complex. Additions of Al to the alloys will in fact decrease the fraction of  $\gamma'$  if the Cr:Al ratio is held constant for alloys of 15% Al - 20% Cr. The influence of Al and Cr on the amount of  $\gamma'$  can be seen to be a function of where the alloy is located in the 2 phase field in relation to the point where the  $\gamma'$  field turns back from the  $\gamma$

field (17% Cr - 13% Al). If one extends this sort of behavior into the multicomponent case, it seems rational to expect that the amount of  $\gamma'$  may be related to the alloy composition through a very complex function which may contain terms of high degree.

The usefulness of equations such as that developed by Decker is not questioned, provided that its use is restricted to alloys close in composition to those used in its development. It appears to this investigator that much more experimental data will be required to develop a functional relation of this type with reliability over a broad range of compositions.

#### Gamma Composition

The composition of  $\gamma$  was calculated for each extraction run for the two phase alloys where sufficient residue could be obtained using the ammonium sulfate base electrolyte. The amount of  $\gamma'$ , its composition and the melt composition were used as input to a mass balance calculation which provided the  $\gamma$  composition. The average composition of the  $\gamma$  in these alloys is shown in Table 12.

The Al varies from 1.9% to 15.4%, the Cr from 6.6% to 30.7% and the Ti varies from 0.0 (not a calculated positive amount) to 3.1%. The non-zero levels of Mo varied from 2.5% to 8.7% and the non-zero amount of W varied from 0.8% to 5.0%. The sample standard deviation for each element is shown in Table 12 and is less than one third the range of the respective element. This suggests that the spread in compositions is significant when compared to the experimental errors.

The compositions in this investigation compare well with those

observed in references 4, 12 and 13. Of the 4 alloys whose  $\gamma$  has the greatest Al content, 3 contain W. This suggests that W may increase the solubility of Al in  $\gamma$  which is consistent with the phase diagram for Ni-Al-W.<sup>6</sup> The one exception contained Mo and no W. Where both Mo and W are present, the maximum Al content of the  $\gamma$  is 7.5% compared to 15.4% when only W is present and 11.8% when only Mo is present. This suggests that the solubility of Al may be related to an interaction between Mo and W. It can also be seen that the largest observed solubility of the refractory elements is for Cr and the solubility was 30.7%. The least observed maximum solubility was of Cr, Mo and W for W and its largest observed solubility was 5.0%. This decrease in solubility is consistent with increasing atomic diameter from Cr to Mo and W. The difference in solubility of Mo and W, however, cannot be explained in this manner.

Comparison of the composition of the  $\gamma$  phase with the composition of the  $\gamma'$  phase (Table 9 and Table 12) indicated that Cr and Mo partition mostly to the  $\gamma$ . Aluminum and Ti partition mostly to  $\gamma'$ . Tungsten appears to partition more in one phase or the other only as a function of composition. On the average it tends to partition toward the  $\gamma'$ , but it does not do so in all the alloys observed.

#### Gamma - Gamma Prime Relationship

The compositions of the  $\gamma$  in Table 12 and  $\gamma'$  shown in Table 9 are compositions of the phases from two phase alloys. These compositions therefore represent points on the solvus hypersurfaces and

when considered in pairs (one  $\gamma$  and one  $\gamma'$ ) from a heat they are, in fact, the compositions of conjugate phases.

To obtain a more useful description of these solvus hypersurfaces, the data points from each extraction were fitted with curves using a multiple linear regression computer program.<sup>45</sup> The model equation used to fit both sets of data was:

$$\begin{aligned}
 Al = & B_0 + B_1 \times Cr + B_2 \times Mo + B_3 \times Ti + B_4 \times W + B_5 \times Cr^2 + \\
 & B_6 \times Mo^2 + B_7 \times Ti^2 + B_8 \times W^2 + B_9 \times Cr \times Mo + \\
 & B_{10} \times Cr \times Ti + B_{11} \times Cr \times W + B_{12} \times Mo \times Ti + \\
 & B_{13} \times Mo \times W + B_{14} \times Ti \times W + B_{15} \times Cr \times Mo \times Ti + \\
 & B_{16} \times Cr \times Mo \times W + B_{17} \times Cr \times Ti \times W + \\
 & B_{18} \times Mo \times Ti \times W + \text{error}
 \end{aligned}$$

where: Al, Cr, Mo, Ti and W are in atomic %

$B_0$  is a constant

$B_1, B_2, \dots, B_{18}$  are coefficients.

For both solvus hypersurfaces, the regression program rejected coefficients with less than a 25% significance level. The low significance level was chosen because it is recognized that the independent variables have error associated with them. Although it is desirable to simplify the equations, the regression analysis assumption that the independent variables are known without error is violated. The low significance level is believed to avoid

rejecting significant terms.

The constant and coefficients for both solvus equations are shown in Table 13. The multiple regression coefficient ( $R^2$ ) for the  $\gamma$  is 0.89 and for the  $\gamma'$ ,  $R^2$  is 0.87.

These two equations may be used to plot sections of the hyper-surfaces or simply to estimate the amount of a particular element in a phase if four others are known. The usefulness of these equations could be increased if they could be used to estimate the compositions of conjugate phases, given the composition of a two phase alloy.

The compositions obtained in this investigation for  $\gamma$  and  $\gamma'$  are the compositions of conjugate phases. Therefore a tie line is known to pass through the  $\gamma$  composition, the alloy composition and the  $\gamma'$  composition. Direction numbers for the tie lines were calculated by:

$$DN_i = \frac{I_\gamma - I_{\gamma'}}{Cr_\gamma - Cr_{\gamma'}}$$

where:  $DN_i$  = direction number for the  $i^{\text{th}}$  element

$I$  = composition of  $I$  in  $\gamma$

$I$  = composition of  $I$  in  $\gamma'$

$Cr$  = composition of  $Cr$  in  $\gamma$

$Cr$  = composition of  $Cr$  in  $\gamma'$

These direction numbers for each element ( $Cr$  being 1.) relate the change in amount of the element along a tie line per unit change in  $Cr$ . These, in effect, describe the slope of the tie lines.

To determine the phase compositions from the alloy composition by using the tie lines, the direction number of the tie line needs to be known as a function of the composition of the alloy. To permit the estimation of the direction numbers from the alloy composition, the NEWRAP program<sup>45</sup> was used to fit the direction numbers for Al, Mo, Ti and W to equations of the form:

$$DN_i = B_0 + B_1 \times Al + B_2 \times Cr + B_3 \times Mo + B_4 \times Ti +$$

$$B_5 \times W + \text{error.}$$

The full model was used for later work because the uncertainties involved in rejecting terms of low significance seemed large when compared to the small gain obtained in simplifying these equations. The values of the constants and coefficients for these equations are summarized in Table 14.

The two phase region of this alloy system can now be described by using the equations for the solvus hypersurfaces and those which relate the direction numbers of the tie lines to the alloy chemistry. In principle, these equations could be solved simultaneously to find the composition of the  $\gamma$  and  $\gamma'$  for an alloy of known composition. This approach was not used because errors resulting from the least squares curve fitting were expected to (and did) result in conditions where the tie lines fail to intersect the solvus hypersurfaces. Furthermore, because the solvuses are parabolic in shape, it is possible that two real and positive solutions exist.

The procedure used to find the compositions of the conjugate

phases from the composition of a two phase alloy is described below. It was programmed in FORTRAN IV for a time-sharing IBM 360 computer. The program is presented in the Appendix. First, the composition of the alloy is used to establish direction numbers for Al, Mo, Ti and W by using the equations from Table 14. Next, the alloy composition is changed by an increment of Cr and the new values for the other elements are calculated from the direction numbers. The composition is therefore still on the tie line. The new values of Cr, Mo, Ti and W are used in the solvus equation to calculate the Al for the solvus, if the other 4 elements were as just estimated. This procedure is repeated until the Al compositions on the tie line and on the solvus agree to within .005% or until it is obvious that no intersection will be found. If it appears that a second solution is likely, the procedure is repeated. If no intersection is located, the closest approach of the tie line to the solvus as defined by the least difference in Al, is displayed as a solution.

To solve for  $\gamma$  composition, the Cr is increased from the alloy composition. To solve for the  $\gamma'$  composition, the Cr is decreased from the alloy composition. The closest approach is taken as a solution if no intersection is found for  $\gamma$  when Al is 0% or Cr is 40%. The closest approach is used for  $\gamma'$  if Al is 30% or Cr is 0%.

The results of this calculation for the two phase experimental alloys are compared to the experimental results in Table 15. Where

two intersections were found, Table 15 shows the higher Cr solution for  $\gamma$  and the lower Cr solution for  $\gamma'$ . These results appeared to be closer to the experimental value. The experimental compositions and those calculated by the phase analysis procedure are in good agreement except for the  $\gamma$  of alloy 14 and alloy 31. It appears that a lower Cr solution was not identified in these two alloys, perhaps because of an accumulation of errors. It should also be noted that alloy 14 had .4% residue with the HCl extraction. The analysis of the phases in this case is more in error than most of the other alloys. However, it is doubted that these errors could be of the size required to explain the difference between the calculated and experimental compositions. No unusual behavior is associated with alloy 31. It appears that the estimation technique is in reasonable agreement with the observed compositions except for two of 50 analyses.

To assist in visualization of the system, a series of quasi-ternary sections were prepared by solving the solvus equations for Al as Cr was varied. The other elements were held constant for a given diagram. This procedure was programmed for the time sharing IBM 360 and the results were plotted using a film plotting procedure. The plot is displayed on a cathode ray tube and is photographed on 35 mm film. These plots were then replotted as an orthographic projection of a solid figure where a third element was varied along an axis perpendicular to the Gibbs triangle. The results of this procedure for an alloy having the composition 8.5 Al, 13.0 Cr, 2.5

Mo, 1.75 Ti, 1.5 W are shown in Figures 6(a), 6(b) and 6(c). The  $\gamma$  for this alloy is expected to have the composition 5.8 Al, 17 Cr, 2.9 Mo, .8 Ti, .5 W and the  $\gamma'$  the composition 15.7 Al, 5.3 Cr, 1.6 Mo, 3.6 Ti, 3.4 W. To prepare Figure 6, the elements which are not varied are held constant at the values expected for the predicted compositions for  $\gamma$  and  $\gamma'$ . For example when Al, Cr and Mo are varied (Fig. 6(a)), the  $\gamma$  has .8 Ti and .5 W; while  $\gamma'$  has 3.6 Ti and 3.4 W. By using this procedure each diagram contains one set of conjugate points.

Figure 6(a) shows that as Mo is increased, the solubility of Al in  $\gamma$  increases slightly at high Cr content, but the Al solubility decreases with increasing Mo at lower Cr content. Additions of Mo to  $\gamma'$  appears to cause the solvus to rotate about an axis near 14 Al and 4 Cr such that at low Mo content the solubility of Al in  $\gamma'$  increases with increasing Cr, but as the Mo is increased this effect reverses. At 4.5% Mo the Al content of  $\gamma'$  is decreased as the Mo is increased.

The effects of Ti additions to  $\gamma$  and  $\gamma'$  are shown in Figure 6(b). Addition of Ti to  $\gamma$  increases the Al solubility at high Cr but lowers it at low Cr. The addition of Ti to  $\gamma'$  appears to decrease the Al solubility at all Cr contents. The decrease in Al solubility is approximately equal to the Ti addition.

Increasing W in the  $\gamma$  causes the solubility of Al to be lowered for a W content above 1% (Fig. 6(c)). From 0 to 1% W the solubility of Al in  $\gamma$  is increased with increasing W. Increasing

W in the  $\gamma'$  causes the Al content to be decreased at a constant Cr. The amount of this reduction in Al solubility is greater at higher Cr content.

Figures 6(d), 6(e) and 6(f) are similar diagrams for an alloy with the same composition, except that it is Mo-free. The alloy composition is 8.5 Al, 13.0 Cr, 1.75 Ti, 1.5 W and Ni is the balance. The expected  $\gamma$  composition is 6.6 Al, 15.7 Cr, 0.9 Ti, 0.7 W and the  $\gamma'$  composition is 9.9 Al, 11.0 Cr, 2.4 Ti, 2.1 W. Comparing Figure 6(a) with Figure 6(d), it is noted that alloying Mo has a similar effect on the Mo-free system as on the Mo-bearing system. Figures 6(b) and 6(e) show that the effect of Ti additions on the  $\gamma'$  are similar for the Mo-free and Mo-bearing compositions. The Al concentration at a given Ti content for the Mo-free  $\gamma$  is greater at low Cr content and lower at high Cr content than for the Mo-bearing  $\gamma$ . The similarity of the effect of W on Mo-free and Mo-bearing alloys is apparent by comparing Figure 6(f) and Figure 6(c). The solubility of Al in Mo-free is greater than in Mo-bearing  $\gamma$  for given Cr and W contents.

The effects of alloying on a W-free composition are shown in Figures 6(g), 6(h) and 6(i). The alloy has a composition of 8.5 Al, 13.0 Cr, 2.5 Mo, 1.75 Ti and the balance is Ni. For this composition the  $\gamma$  is expected to be 3.8 Al, 18.8 Cr, 2.9 Mo, with the balance as Ni; the  $\gamma'$  is 12.8 Al, 7.8 Cr, 2.1 Mo, 3.4 Ti, balance Ni. Comparison of Figures 6(g), 6(d) and 6(a) indicates the similar behavior when Mo is added. At high Mo, however, the W-free  $\gamma$

has a lower solubility for Al at high Cr contents than the W-bearing  $\gamma$  phase. Titanium additions effect the W-free phases in essentially the same manner as it affects the W-bearing phases. This similarity is shown by comparing Figures 6(h), 6(a) and 6(b). The effects of W additions to W-free phases are indicated in Figure 6(i). The general effects are similar to those previously noted for phases bearing W and Mo (Figs. 6(c) and 6(f)). The greatest difference is the low solubility that the W-free  $\gamma$  has for Al at high Cr content. At low Cr contents, W additions increase the solubility of Al in  $\gamma$ .

It is pointed out that the tie lines do not usually fall in the volume of these figures. This type of presentation is intended only to assist in visualizing the influence that alloying has on the system. For greater details concerning the composition of conjugate phases, mathematical models of the type shown in the Appendix are required. It is further noted that the investigator knows of no fundamental basis for the model equations used to fit the solvus hypersurfaces or the direction number equations for the tie lines. It should be recognized that a large number of functions should be capable of describing this system. The author restricted his work to the use of low degree functions of simple polynomials.

The functions selected have been shown to be capable of describing an isothermal section of the Ni-Cr-Al-Ti-Mo-W system where  $\gamma$  and  $\gamma'$  are conjugate phases. This was accomplished by preparing essentially the same number of melts as reported in reference 3 where a quaternary portion of the system was studied

and tie lines were not made available.

#### Lattice Parameters of Gamma and Gamma Prime

The lattice parameters of  $\gamma$  and  $\gamma'$  for the experimental alloys are shown in Table 7. The values observed compare well with those obtained in other investigations<sup>3,4,8,10,11</sup> where three or more components were studied.

The lattice parameter data shown in Table 7 was fitted to the linear equation suggested by Loomis.<sup>4</sup> The results of the regression analysis are summarized in Table 16. The multiple correlation coefficient ( $R^2$ ) is 0.74 for  $\gamma$  and 0.66 for  $\gamma'$ . The value of the coefficients for relating the lattice parameter and composition of  $\gamma$  were found to be smaller than those proposed by Loomis.<sup>4</sup> Except for the coefficient for Ti, which is not significant at a high level in this investigation, the relation between the other coefficients is comparable in both studies. For example Mo and W have essentially the same effect on the lattice parameter of  $\gamma$  and Cr is only about one-fourth as effective as Mo or W in changing the lattice parameter. The results of using Loomis's<sup>4</sup> equation on data from this study are shown in Figure 7(a). It can be seen that Loomis's equation is effective in predicting the lattice parameter of  $\gamma$  for this study. Only two data points fall outside of  $3\sigma$  limits based on the regression analysis performed in this study.

Loomis<sup>4</sup> assumed that the same coefficients used to calculate the  $\gamma$  lattice parameter could also be used to estimate the lattice parameter of  $\gamma'$ . The only difference in his two equations was in

that the constant used to estimate the lattice parameter of  $\gamma'$  was  $0.0032 \text{ \AA}^\circ$  smaller than for  $\gamma$ . The agreement between his equation and the one developed from data in this study is not as good as for determining the lattice parameter of  $\gamma$  (Table 16). Both investigations show that Mo and W are equally effective in changing the lattice parameter of  $\gamma'$ . This study suggests that Ti is slightly more effective than Mo and W in changing the lattice parameter of  $\gamma'$ , while Loomis<sup>4</sup> suggested that Ti was slightly less effective than Mo and W in changing the lattice parameter of  $\gamma'$ . Loomis<sup>4</sup> suggested that Al and Cr additions expand the  $\gamma'$  lattice, whereas this investigation suggests the opposite is true. The magnitude of the coefficients determined in this study are about 1/10th the magnitude of those used by Loomis. The results of applying Loomis's equation to the  $\gamma'$  data of this investigation are shown in Figure 7(b). Five predictions fall outside of the  $3\sigma$  limits based on the regression analysis performed in this study.

Since the equations developed in this study were based on the data obtained in this study, these equations predict the behavior of this data better than the equations of Loomis. If one considers that the simplest alloys examined in this investigation were quaternary alloys and that Loomis used binary data to develop his equations, the agreement in the equations is remarkable. The equations developed in this study used only the compositions of phases at the phase boundaries, whereas the earlier study used mostly single phase alloys. Because the lattice parameters and chemical analyses in the earlier

were taken from bulk samples, the prediction of lattice parameter from chemical analysis should be more accurate. The present work tends to account for possible interactions among the elements and reflects the rather constant lattice parameter of the  $\gamma'$ . This constant parameter, results from the fact that the composition of  $\gamma'$  at the phase boundary is relatively constant as compared to  $\gamma$  at its phase boundary.

The standard error of the estimate ( $\sigma$ ) is shown in Table 16 to be 0.0043  $\text{Å}^\circ$  for the lattice parameter of  $\gamma$  and 0.0026  $\text{Å}^\circ$  for estimating the lattice parameter of  $\gamma'$ . If these equations were used to determine the lattice mismatch, the standard error of the mismatch would be 0.0069  $\text{Å}^\circ$  or approximately 0.2% of the parameter. This standard error is of the magnitude of the mismatch observed in many alloys, therefore it is of questionable value as an alloy development tool. It is not known whether a more complex model can substantially reduce the standard error and be more capable of estimating the lattice mismatch in alloys, but it does appear that a large amount of the error results from chemical analysis where the standard deviation of Mo and W (the two most effective elements for changing the lattice parameter of  $\gamma$ ) are 0.224 and 0.374. These standard deviations are 5 - 10% of the mean analysis for these elements.

#### Degree of Order in Gamma Prime

The long range order parameter (S) was calculated for those  $\gamma'$  compositions for which the intensity of the (100) reflection

could be measured and for which the chemical composition of the  $\gamma'$  was known. The data used to determine the long range order parameter (S) was the X-ray data from Table 7 and the composition of  $\gamma'$  shown in Table 9. The order parameter (S) was taken as the square root of the ratio of the measured intensity ratio ( $I_{100}/I_{200}$ ) to the calculated value of the same ratio. For the calculated intensity ratio value, the chemical formula shown in Table 17 was assumed for the  $\gamma'$ . The intensity ratio was calculated using the computer program POWD2.<sup>42</sup> The long range order parameter (S) is shown in Table 17.

The long range order parameter was least squares fitted to a linear equation in terms of the composition of the  $\gamma'$ . The resulting equation:

$$S = 1.08 - .024 \text{ Al} - .0070 \text{ Cr} + .0051 \text{ Mo} - .015 \text{ Ti} + .096 \text{ W}$$

where S = long range order parameter

Al, Cr, Mo, Ti and W = at. % in  $\gamma'$

had a multiple regression coefficient ( $R^2$ ) of 0.79. The coefficients for Al, Ti and W were significant at greater than 0.95, whereas the coefficients for Mo and Cr were not significant at 0.51.

The results of this analysis were anticipated since Cr and Mo have scattering factors not substantially different from Ni and the range of composition of Cr and Mo in  $\gamma'$  is small.

Increasing W increases the order parameter probably because it was assumed to occupy Al sites in preference to Ni sites. If W is

assumed to occupy only Al sites, the calculated intensity ratio will be at a minimum. If W has the tendency to occupy Ni sites, the observed intensity ratio will tend to be greater than the calculated intensity ratio. Therefore the presence of W will appear to increase the long range order parameter even though the actual order is decreased. These data are interpreted to indicate that the order of the  $\gamma'$  decreases as the alloy content is increased. However specific details are masked because it is not obvious how to define the fully ordered state for a 4 - 6 component phase.

#### Occurrence of Other Phases

Phases other than  $\gamma$  and  $\gamma'$  were identified in 22 alloys. The phases observed were sigma, mu and 2 body-centered-cubic phases. One body-centered-cubic phase had a lattice parameter similar to Cr and the other had a lattice parameter similar to Mo and W. Table 6 lists the alloys, the phases observed in the alloys and the amount of residue collected with HCl and ammonium sulfate electrolytes. Table 18 summarizes the occurrence of the phases and the compositions of the alloys.

Inspection of Table 18 reveals that only 2 alloys (3 and 44) contain more than 70% Ni. No alloy which formed phases other than  $\gamma$  and  $\gamma'$  had more than 75% Ni. Five of the alloys (15, 31, 37, 38 and 49) which formed either only  $\gamma$  or  $\gamma$  and  $\gamma'$  had less than 70% Ni (converted to atomic % from the data in Table 2). All of these alloys which formed either just  $\gamma$  or  $\gamma$  and  $\gamma'$  had more than 65% Ni. It appears that alloys with greater than 75% Ni will

not form phases other than  $\gamma$  and  $\gamma'$ , while alloys with less than 65% Ni are virtually guaranteed to form additional phases. This compares well with the observations reported in reference 35 showing the  $\gamma$  to  $\gamma + \sigma$  boundary to lie between 64 and 61% (Ni + Co) at 843° C and also compares well with reference 9 which shows the  $\gamma$  to  $\gamma + \alpha$  boundary to be essentially constant at 60% Ni at 850° C. Reference 9 also shows that for the  $\gamma + \gamma'$  to  $\alpha + \gamma + \gamma'$  boundary at 850° C, the Ni is nearly constant at 62%.

The compositions of the alloys shown in Table 18 were used to estimate the compositions of  $\gamma$  and  $\gamma'$  using the computer program shown in the Appendix. It was observed that the Al direction number ( $dAl/dCr$ ) was greater than 0. for 8 alloys. This occurrence was not observed for the 2 phase alloys where the greatest value for the Al direction number was -0.22. Thirteen of the multiphase alloys were observed to have Al direction numbers greater than -0.20. Referring to Figure 2, it can be seen that the slope of the tie lines between  $\gamma$  and  $\gamma'$  tend to rotate toward higher Al:Cr ratios as the Cr is increased and the two phase to three phase boundary is approached. The boundary between  $\alpha + \gamma$  and  $\alpha + \gamma + \gamma'$  does in fact have a slope such that Al:Cr is approximately -0.2. The use of the Al direction number as a measure of whether phases other than  $\gamma$  and  $\gamma'$  may form in the alloys can in part be justified from the ternary phase diagram shown in Figure 2.

It is assumed that alloys having less than 67% Ni will form phases other than  $\gamma$  and  $\gamma'$ ; and that alloys with Al direction

numbers greater than -0.2 also form phases other than  $\gamma$  and  $\gamma'$ . When the presence of the phases observed are compared with these assumptions, these assumptions are followed except for alloys 3, 4, 9, 13 and 44, which would not be expected to form phases other than  $\gamma$  and  $\gamma'$ , but do and for alloy 15 (65.5% Ni) which would be expected to form phases other than  $\gamma$  and  $\gamma'$ , but does not.

Two additional assumptions: first, that the same compositional limit for two phase alloys applies to just the  $\gamma$  phase of the alloy, or that phases other than  $\gamma$  and  $\gamma'$  will form if  $\gamma$  has Ni less than 67% and, second, that Mo and W are 1.75 more potent than Cr in promoting additional phases,<sup>35</sup> can be made. Under these conditions additional phases should be expected if  $\text{Cr} + 1.75 (\text{Mo} + \text{W})$  is greater than 33. Adding these assumptions to the two previous ones leaves only alloys 4 and 44 that were multiphase when expected to be two phase, and alloys 15 and 35 which were two phase when expected to be multiphase alloys.

The composition of the HCl extraction residues from selected heats are shown in Table 19. The X-ray diffraction pattern for heats 17 and 24 were those for Cr. Table 19 shows that the residues from these heats contain in excess of 91% Cr. Small amounts of Ti, Ni, and Zr were found in the residues. The Zr was not intentionally added to the melt and probably came from the zirconia crucibles. The composition of these residues is taken as confirmation that the diffraction pattern is that of the Cr terminal solid solution as compared with an intermediate beta phase which could have a similar

X-ray diffraction pattern, but would have substantially higher Ni contents (25% minimum).

The composition of the mu phase extracted from heats 13 and 42 suggest a formula of  $(Ni_aCr_b)(Cr_cMo_dW_eTi_f)$  for the phase. The Al content was neglected because of its low level. The compositions of the residues from heats 9 and 45 are consistent with the phase analyses. Heat 44 appears from the chemical analysis to be intermediate in composition to alloys 13 and 45, except for the higher W content in 44. It is therefore assumed that heat 44 contains mu and W phases. The presence of sigma phase appears unlikely because Kirby<sup>35</sup> reported sigma phase to have approximately 55% Cr. The Cr in the residue from alloy 44 is low.

Table 18 also shows that no alloys were observed to contain both Cr and mu. This same mutual exclusion can also be noticed in reference 34. No other possible multiphase fields were absent but the previously noted exception excludes the existence of fields containing more than 5 phases. The reduced phase rule would suggest that 6 phase fields might be observed. (It is assumed that the invariant point of 7 phases cannot be observed in this type of experiment.)

#### Morphology of Phases

Gamma and Gamma Prime-Scanning electron micrographs of selected alloys are shown in Figure 8. The darker phase in the micrographs is believed to be  $\gamma'$ . The amount, shape and size of the  $\gamma'$  can be seen to vary widely. None of these variations could be correlated

with specific alloy elements or the composition of the alloy.

References 4 and 21 suggest that a correlation exists between the  $\gamma - \gamma'$  lattice mismatch and the shape of the  $\gamma'$ . Specifically, reference 4 suggests that at a lattice mismatch near  $0.005 \text{ \AA}^\circ$ , the  $\gamma'$  is round. Changing the mismatch causes the  $\gamma'$  to become "globular", then "blocky" and at a mismatch of approximately  $0.003 \text{ \AA}^\circ$  the  $\gamma'$  shape is described as square. The range of mismatch observed in reference 4 was  $-0.02$  to  $0.03 \text{ \AA}^\circ$ . The range of mismatch in this investigation varied from  $-0.013$  to  $0.028 \text{ \AA}^\circ$ , but no strong correlation between  $\gamma'$  shape and lattice mismatch was observed. An example of round  $\gamma'$  is shown in alloy 33 (Fig. 8(a)) where the mismatch is unknown. The  $\gamma'$  in alloy 39, where the mismatch is  $0.001 \text{ \AA}^\circ$ , is "globular" (Fig. 8(b)). The distinction between "blocky" and square was somewhat vague in reference 4, but the  $\gamma'$  in alloy 99 (Fig. 8(c)) is similar to what Loomis<sup>4</sup> called "square" while the  $\gamma'$  in alloy 37 (Fig. 8(d)) could be "blocky".

Examples of primary  $\gamma'$  are shown in Figures 8(e) and 8(f). The regions of large  $\gamma'$  with a "kidney" or rounded shape are believed to have formed directly from the liquid. The coarse  $\gamma'$  adjacent to the primary  $\gamma'$  is typical of that which precipitates at high temperatures. The very fine  $\gamma'$  is typical of that which precipitates at low temperatures and is assumed to have precipitated during the  $850^\circ \text{ C}$  aging treatment.

Figures 8(c) and 8(d) show  $\gamma'$  particles which have precipitated in grain boundaries. In commercial alloys carbide precipita-

tion is usually observed to occur at grain boundaries. The  $\gamma'$  which is observed at the grain boundaries in the commercial alloys is commonly associated with the carbide precipitation.

The two  $\gamma'$  sizes in alloy 7 varied in diameter by approximately 30 times (Figs. 8(g,h)). The fine  $\gamma'$  appears "blocky", but the coarse  $\gamma'$  appears to be "globular". Following the reasoning of reference 4, one would assume that the lattice mismatch is different for the two shapes (sizes). There was no evidence of this occurrence in the X-ray diffraction patterns.

Additional Phases - Figure 9 shows micrographs selected to show the morphology of the phases other than  $\gamma$  and  $\gamma'$  which were observed in this study. The body-centered-cubic phase which is an Mo-W solid solution could be easily observed in the unetched specimens. Figure 9(a) shows alloy 4 unetched. This alloy contained only W, and  $\gamma'$ , therefore the phase observed in the unetched specimen can be assumed to be W. The same phase in alloy 6 has a "chinese script" shape (Fig. 9(b)). In alloy 10 (Fig. 9(c)) the phase is similar to that in alloy 6 except that it is slightly finer. In alloy 25 (Fig. 9(d)) the W phase is a rather coarse interdendritic phase.

The W phase in alloy 8 is shown in Figure 9(e). This phase appears as a dark star like figure with a ring around it. Microprobe analysis of this morphology indicated that the core region of the star was very rich in W and Mo, but low in Cr, Al, and Ti. The ring was rich in Cr, but low in the other elements. X-ray diffraction

analysis of this alloy indicated that both the Cr and W phases were present. The structure is believed to show a W-Mo solid solution which is coated with a Cr solid solution. Although the miscibility gap between (W,Mo) and Cr<sup>46,47</sup> is normally thought to be a solid state reaction, the morphology shown here suggests that the miscibility gap manifests itself as a peritectic reaction in these alloys.

The Cr phase was normally visible in unetched specimens such as seen in Figure 9(e), but it was difficult to obtain sufficient contrast to prepare suitable micrographs. This phase could be easily detected when the specimen was etched with KOH. The phase can be seen as fine particles in alloy 17 (Fig. 9(f)), and in alloy 24 (Fig. 9(g)). The very fine precipitate in alloy 17 can be seen to be needles in a scanning electron micrograph (Fig. 9(h)).

It appears that the Cr phase may precipitate either from the liquid as in alloy 8 or in the solid state as in alloys 17 and 24. In the solid state a plane of coherency can easily be established between the (110) of Cr and the (200) of the Ni rich solid solution. The X-ray diffraction patterns of these phases show these lines to be almost coincident.

The presence of sigma and mu phases could only be established in etched samples. The mu phase appeared as fine particles in the grain boundaries and as needles or plates in the grains. Examples of mu phase in alloy 3 (Fig. 9(i)) shows the appearance of mu in a sample with little of the phase present. Figure 9(j) shows the appearance of mu phase in alloy 13 which contained a larger amount

of the phase.

The sigma phase appeared as fine plates or needles and could not be distinguished from mu phase. Figure 9(k) shows alloy 6 etched with KOH. The "chinese script" is W and the fine plates or needles are sigma phase.

The morphology of the sigma and mu phases suggest that they have precipitated in the solid state. It is assumed that they precipitated at the 950° C aging temperature which has been shown to be near the temperature of maximum precipitation rate in commercial alloys.<sup>6,29,30,33</sup> The morphology of these phases appear the same in this investigation as in several studies of commercial Ni-base superalloys.<sup>16,27-33</sup>

#### Application to Commercial Alloys

The composition and heat treatment of the alloys from reference 12 are shown in Table 20. These alloys are typical of current commercial Ni-base superalloys. The heat treatments for the alloys, except for Udimet 700, are typical of the condition in which the alloys may be placed in service.

In addition to the 6 elements studied in this investigation, it can be seen that the commercial alloys contain C and may have intentional additions of Co, Nb, Fe, Ta and V. These alloys usually have 0.01 - 0.05 wt. % B although it was not reported in reference 12.

The compositions from Table 20 were used to determine whether the "phase diagram" from this investigation could be applied to commercial alloys. The tests for additional phase formation were

also applied to these alloys. Finally the reported lattice parameter of  $\gamma'$  for these alloys is compared with a predicted one.

To test the "phase diagram", the compositions from Table 20 were first converted to atomic percent. The composition was then adjusted for carbide formation by using the procedures suggested in reference 19. The adjusted composition was then treated as an alloy composition using the program in the Appendix. The procedure in effect treated all elements other than Al, Cr, Mo, Ti and W as if they were Ni. This appears to be a reasonable assumption for Co and Fe, but Ta and Nb are shown in reference 12 to be  $\gamma'$  formers.

The results of these calculations of  $\gamma$  and  $\gamma'$  composition are compared to the compositions reported in reference 12 in Table 21. The compositions of  $\gamma$  calculated compare well with those reported except for alloys IN 100, Mar M 200, Nimonic 115 and Nicrotung. For the  $\gamma'$  compositions, only alloys Inconel X-750 and Unitemp AF 1753 failed to show good agreement between the calculated and observed values. For alloy Unitemp AF 1753, the estimating procedure reported the alloy composition for the  $\gamma$  composition. This can be considered to indicate the alloy to be single phase.

The "phase diagram" of this investigation is able to usefully describe one phase in all of the commercial alloys examined. Of the six phase analyses which were not in reasonable agreement, four were for the  $\gamma$  phase. This is probably because it was the  $\gamma'$  composition which was directly determined in both this investigation and reference 12. A greater uncertainty should therefore exist concern-

ing the composition of the  $\gamma$  phase. For the two alloys for which the  $\gamma'$  estimate was poor, it can be seen in Table 1(a) that they had the lowest weight fraction  $\gamma'$  of the alloys examined. Errors in estimating the tie line direction numbers would be expected to be seen as an error in the composition of the phase more distant from the alloy composition because of a leverage effect. This is what is observed.

The results of the above comparisons indicate that the techniques developed in this investigation should be capable of being adapted for use in commercial alloys. It appears that the discrepancies between the estimates based on the current work and reference 12 are partly the result of the fact that the alloys in reference 12 were heat treated for shorter times and at different temperatures than the current work. The other obvious source of differences is that the current work made no attempt to account for additional elements, except as they enter into carbide reactions.

Because the formation of phases such as sigma and mu have been correlated with undesirable changes in mechanical properties,<sup>16,27-33</sup> it is desired to be able to predict their formation. It was observed in this investigation that alloys having the following were likely to form phases other than  $\gamma$  and  $\gamma'$ : less than 67% Ni in the alloy;  $\gamma$  greater than  $33\text{Cr} + 1.75(\text{Mo} + \text{W})$  or an Al direction number greater than 0.2. To examine the commercial alloys reported in reference 12, it was assumed that the sum  $\text{Ni} + \text{Co} + \text{Fe}$  could be substituted for Ni in the 67% rule. Although the occurrence of

additional phases was not reported in reference 12, the same commercial compositions, except GMR 235, were evaluated relative to the formation of additional phases in reference 16. It is recognized that the compositions of the specific alloys may be somewhat different but the relative tendency toward additional phase formation should be similar between the alloys in references 12 and 16.

The three parameters used to evaluate the alloys are summarized in Table 22. No alloy with greater than 69% Ni + Fe + Co formed sigma or mu phase. The alloys which formed sigma or mu had a  $\gamma$  phase which had more than 29.2 Cr + 1.75 (Mo + W). Of the alloys which had an Al direction number greater than -0.3, only Nicrotung did not form sigma or mu phase.

It appears that the critical points for establishing if an alloy will form phases other than  $\gamma$  and  $\gamma'$  are slightly different for the alloys in reference 12 than for the alloys in this study. The stability trends, however appear to be the same for both sets of alloys. The differences may result partly from the fact that the alloys in reference 16 were aged 1500 hours at 871° C and that the compositions of the alloys in reference 16 are different from those in reference 12. This investigator has probably over-simplified the treatment of the elements not included in this investigation, but it appears that the basis for determining if additional phases will occur in Ni-base superalloys proposed here can be easily related to commercial alloys.

The lattice parameter of the  $\gamma'$  for the alloys in reference

12 were estimated using the  $\gamma'$  compositions from reference 12 and the regression coefficients from reference 4. The regression coefficients from this investigation were not used because the coefficients for Co, Fe and Nb are not known. The estimated parameters are compared to the lattice parameters reported in reference 12 in Table 23. It is evident that the equation proposed by Loomis<sup>4</sup> is capable of estimating the lattice parameter of  $\gamma'$  in commercial alloys. Only Mar M 200 of the 12 alloys for which all the required regression coefficients were known, exhibits a difference between the observed and estimated parameters over 0.003 A°.

It has been shown that the phase relationship between  $\gamma$  and  $\gamma'$  identified in the current work for a 6 component (Ni-Cr-Al-Ti-Mo-W) system at 850° C appears to be generally appropriate for commercial Ni-base superalloys. Three simple parameters which are available from the current work appear capable of estimating whether phases such as sigma or mu will form in the commercial alloys. This work and reference 4 have shown that the lattice parameters of  $\gamma'$  in commercial alloys can be estimated using regression coefficients derived from simple systems. Because the coefficients used to estimate the  $\gamma$  lattice parameter are similar to those for  $\gamma'$ , it is assumed the estimates obtained for both phases should be equally reliable. Although this technique currently does not show the degree of accuracy required to exploit its use in alloy design, the potential of the approach is clearly established.

It is suggested that by coupling the data of this investigation

with data to account for the behavior of C, Nb, V, Hf, and Ta, the more obvious sources of errors can be taken into account. It appears that Co and Fe are not now a major source of error since they appear to behave much the same as Ni in the commercial alloys studied in reference 12.

## V SUMMARY AND CONCLUSIONS

Fifty one Ni-base alloys were melted and heat treated for 4 hours at 1190° C followed by 1008 hours at 850° C to obtain information on the manner in which some of the more important alloying elements in Ni-base superalloys are partitioned between  $\gamma$  and  $\gamma'$  phases. The Ni-base alloys were prepared with variations of the alloying elements over the following nominal ranges: Al 4.0 to 13 atomic %, Cr 6.5 to 20.5%, Ti 0.25 to 4.75%, Mo 0.0 to 6.0% and W 0.0 to 4.0%. The object of the investigation was to produce a mathematical model of the Ni-rich region of the Ni-Al-Cr-Ti-Mo-W system at 850° C.

The following conclusions result from this investigation.

(1) It was determined that  $\gamma'$  had the following range of compositions for the various elements contained in this phase:

Ni	72.1 to 78.0 atomic %
Al	7.8 to 17.3%
Cr	1.5 to 8.9%
Ti	0.3 to 13.9%
Mo	0.0 to 3.9%
W	0.0 to 7.2%

The Ni varied only slightly from the 75% which is the correct stoichiometric ratio for  $Ni_3Al$ .

(2) The composition of the  $\gamma$  determined experimentally varied

as follows:

Ni is balance

Al 1.9 to 15.4 atomic %

Cr 6.6 to 30.7%

Ti 0.0 to 3.1%

Mo 0.0 to 8.7%

W 0.0 to 5.0%

W additions to the  $\gamma$  appeared to increase the solubility of Al slightly in the  $\gamma$ . Mo and W added together decreased the solubility of Al in  $\gamma$  and the effect appeared to be greater than the reduction of Al solubility observed when only Mo was present.

(3) Equations of the third degree based on the experimental data were fit to the solvus hypersurfaces. The multiple correlation coefficients ( $R^2$ ) were relatively good for these equations: 0.87 for the  $\gamma$  and 0.89 for the  $\gamma'$ . A computer program was written to determine the composition of  $\gamma$  and  $\gamma'$  by locating the intersection of the tie line of a two phase alloy and the solvus hypersurfaces. This program was based on the equations of the solvus hypersurfaces and an experimentally determined relationship between the alloy composition and direction numbers for tie lines. The phase compositions calculated by this program agreed well with experimental observations for 48 out of 50 analyses of the resulting phases. The same program could be applied to commercial Ni-base superalloys and yield satisfactory agreement with reported phase analyses for 24 out of 30 analyses.

(4) The elements Al and Ti partitioned more to the  $\gamma'$  than to the  $\gamma$ . Mo and Cr partitioned more to  $\gamma$  than to  $\gamma'$ . Tungsten partitioned more to one phase than the other only as a function of the alloy composition.

(5) The amount of  $\gamma'$  varied from 0.0 to 55.7 weight %. The amount of  $\gamma'$  could not be correlated to the composition of the alloy using equations of 1<sup>st</sup> to 3<sup>rd</sup> degree.

(6) The results of the X-ray diffraction studies indicated that the lattice parameter of both  $\gamma$  and  $\gamma'$  could be estimated from the phase composition using 1<sup>st</sup> degree linear equations. This form of equation predicted the lattice parameters for  $\gamma'$  in commercial Ni-base superalloys which were in good agreement with published values.

(7) Phases other than  $\gamma$  and  $\gamma'$  were observed in this investigation. Two body-centered-cubic phases, one appearing to be a Cr terminal solid solution and the other a Mo-W solid solution were identified. Sigma and mu phases were also identified in some alloys. The Cr solid solution and mu were never observed to occur as conjugate phases.

(8) Experimental alloys with less than 67 atomic % Ni, or for which the quantity  $(Cr + 1.75 (Mo + W))$  was greater than 33 are very likely to form phases other than  $\gamma$  and  $\gamma'$ . In addition, when the Al direction number  $(dAl/dCr)$  of the tie line was greater than -0.2, the alloy is very likely to form phases other than  $\gamma$  and  $\gamma'$ . It appears that these same criteria with minor modifications may be applicable to commercial Ni-base superalloys.

(9) The investigation has demonstrated that a two phase field of a 6 component system can be mathematically modeled. With the aid of a digital computer, the model can be examined to provide the same information that is available in isothermal sections of classical phase diagrams. In addition to the phases present, the lattice parameters of these phases can be determined from the phases' compositions.

#### REFERENCES

1. R. J. Quigg and H. E. Collins, Superalloy Development for Aircraft Gas Turbines, presented at the Gas Turbine Conference & Products Show, Cleveland, Ohio, March 9-13, 1968, ASME paper 69-GT-7.
2. William J. Boesch and John S. Slaney, "Preventing Sigma Phase Embrittlement in Nickel Base Superalloys," Metals Progress, vol. 86, no. 1, July 1964, 109-111.
3. A. Taylor, "Constitution of Nickel-Rich Alloys of the Ni-Cr-Ti-Al System," Trans. AIME, vol. 206, Oct. 1956, 1356-1362.
4. Warren T. Loomis, "The Influence of Molybdenum on the  $\gamma'$  Phase Formed in a Systematic Series of Experimental Nickel-Base Superalloys" (Unpublished PhD Dissertation, University of Michigan, 1969).
5. Andrej Havalda, "Influence of Tungsten on the  $\gamma'$  to  $\eta$  Transformation and Carbide Reactions in Nickel-Base Superalloys," Trans. ASM, vol. 62, 1969, 581-589.
6. "Binary and Ternary Phase Diagrams of Columbium, Molybdenum, Tantalum, and Tungsten (Supplement to DMIC Report 152)" Defense Metals Information Center Report 183, Batelle Memorial Institute, Columbus, Ohio, February, 1963.

7. R. W. Guard and E. A. Smith, "Constitution of Nickel-Base Ternary Alloys," J. Inst. Met., vol. 88, 1959, 283.
8. A. Taylor and R. W. Floyd, "The Constitution of Nickel-Rich Alloys of the Nickel-Chromium-Aluminum System," J. Inst. Met., vol. 81, 1952-53, 451-464.
9. C. M. Hammond, R. A. Flinn and Lars Thomassen, "Phase Equilibria and Elevated-Temperature Properties of Some Alloys in the System  $\text{Ni}_3\text{Cr-Ni}_3\text{Al}$ ," Trans. AIME, vol. 221, April 1961, 400-405.
10. A. Taylor and R. W. Floyd, "The Constitution of Nickel-Rich Alloys of the Nickel-Titanium-Aluminum System," J. Inst. Met., vol. 81, 1952-53, 25-32.
11. A. Taylor and R. W. Floyd, "The Constitution of Nickel-Rich Alloys of the Nickel-Chromium-Titanium System," J. Inst. Met., vol. 80, 1951-52, 577-587.
12. Owen H. Kriege and J. M. Baris, "The Chemical Partitioning of Elements in Gamma Prime Separated from Precipitation-Hardened, High-Temperature Nickel-Base Alloys," Trans. ASM, vol. 62, March 1969, 195-200.
13. J. R. Mihalisin and D. L. Pasquine, "Phase Transformations in Nickel-Base Superalloys," AIME International Symposium on Structural Stability in Superalloys, Seven Springs, Penna., Sept. 4-6, 1968, 134-171.
14. N. I. Blok, A. I. Glazova, M. N. Kozlova, N. F. Lashko, G. I. Morozova, and K. P. Sorokina, "Comparison of Methods of Separating Phases in Nickel-Chromium Alloys," Spektal'nyye i

- Khimicheskiye Metody Analiza Materialov, Sbornik Metodik, Izd-vo Metallugiya, Moscow, 1964, 78-83, translated by E. Harter, Translation Div., Foreign Technology Div., WP-AFB, Ohio.
15. L. R. Woodyatt, C. T. Sims, and H. J. Beattie, Jr., "Prediction of Sigma-Type Phase Occurrence from Composition in Austenitic Superalloys," Trans. AIME, vol. 236, no. 4, April 1966, 519-527.
  16. H. E. Collins, "Research on Microstructural Instability of Nickel-Base Superalloys," Technical Report AFML-TR-68-256, Air Force Materials Laboratory, Air Force Systems Command, Wright-Patterson Air Force Base, Ohio, 1968.
  17. R. L. Dreshfield, "A Proposed Method for Estimating Residual Matrix Chemistry in Nickel-Base Superalloys," NASA TM X-52530, 1969.
  18. R. L. Dreshfield, "Estimation of Gamma Phase Composition in Nickel-Base Superalloys," Met. Trans., vol. 2, May 1971, 1341-1346.
  19. R. F. Decker, "Strengthening Mechanisms in Nickel-Base Superalloys," Paper presented at Steel Strengthening Mechanisms Symposium, Zurich, Switzerland, May 5-6, 1969, sponsored by Climax Molybdenum Company.
  20. W. C. Hagel and H. J. Beattie, Jr., "Cellular and General Precipitation During High Temperature Aging," Iron and Steel Institute, Special Report Number 64, 1959, 98-107.

21. R. G. Davies and T. L. Johnston, "The Metallurgical Design of a Superalloy," Paper presented at Third Bolton Landing Conference on Intermetallic Compounds, Their Alloys, Ordering and Physical Metallurgy, Bolton Landing, New York, Sept. 8-10, 1969.
22. R. F. Decker and J. R. Mihalisin, "Coherency Strains in  $\gamma'$  Hardened Nickel Alloys," Trans. ASM, vol. 62, 1969, 481-489.
23. G. N. Maniar, J. E. Bridge, H. M. James and G. B. Heydt, "Correlation of Gamma-Gamma Prime Mismatch and Strengthening in Ni/Fe-Ni Base Alloys Containing Aluminum and Titanium as Hardeners," Met. Trans., vol. 1, Jan. 1970, 31-42.
24. S. M. Copley and B. H. Kear, "A Dynamic Theory of Coherent Precipitation Hardening with Applications to Nickel-Base Superalloys," Trans. AIME, vol. 239, 1967, 984.
25. W. G. Dorfeld and V. A. Phillips, "The Extent of Long-Range Order in  $\gamma'$  Particles Extracted from René 63 Superalloy," Metallography, vol. 3, 1970, 285-289.
26. J. R. Mihalisin, "Measurement of Long Range Order in the  $\gamma'$  Phase of Nickel-Base Superalloys," presented at 18th Denver X-ray Conference, 1969.
27. S. T. Wlodek, "The Structure of IN-100," Trans. ASM, vol. 57, no. 1, March 1964, 110-119.
28. International Symposium on Structural Stability in Superalloys, Seven Springs, Penna., Sept. 4-6, 1968.
29. R. L. Dreshfield and R. L. Ashbrook, "Sigma Phase Formation and

- Its Effect on Stress-Rupture Properties of IN-100," NASA TN D-5185, 1969.
30. R. L. Dreshfield and R. L. Ashbrook, "Further Observations on the Formation of Sigma Phase in a Nickel-Base Superalloy (IN-100)," NASA TN D-6015, 1970.
  31. E. W. Ross, "René 100: A Sigma-Free Turbine Blade Alloy," J. Metals, vol. 19, no. 12, Dec. 1967, 12-14.
  32. C. T. Sims, "A Contemporary View of Nickel-Base Superalloys," J. Metals, vol. 18, no. 10, Oct. 1966, 1119-1130.
  33. J. R. Mihalisin and C. G. Bieber, "Sigma - Its Occurrence, Effect, and Control in Nickel-Base Superalloys," Trans. AIME, vol. 242, no. 12, Dec. 1968, 2399-2414.
  34. H. J. Beattie, Jr. and W. C. Hagel, "Compositional Control of Phases Precipitating in Complex Austenitic Alloys," Trans. AIME, vol. 233, no. 2, Feb. 1965, 277-287.
  35. G. N. Kirby, "The Relative Effects of Chromium, Molybdenum, and Tungsten Upon the Occurrence of Sigma Phase Precipitate in Nickel-Base Alloys," Ph.D. Dissertation, University of Michigan, 1971.
  36. O. S. Ivanov, "Algebraic Method of Representing the Phase Diagrams of Many-Component Systems," Izvest. Akad. Nauk SSSR, Metally no. 1, Jan.-Feb. 1969, 204-209.
  37. W. S. Connor and M. Zelen, "Fractional Factorial Experiment Designs for Factors at Three Levels," National Bureau of Standards Applied Mathematics Series No. 54, Washington, D.C.:

- Government Printing Office, 1959, 12.
38. R. L. Dreshfield, "Estimation of Gamma Phase Composition in Nickel-Base Superalloys (Based on Geometric Analysis of a Four-Component Phase Diagram)," NASA TN D-5783, Washington, D.C., May 1970, 16-18.
  39. W. A. Gordon and G. B. Chapman, "Quantitative Direct-Current Arc Analysis of Random Compositions of Microgram Residues in Silver Chloride Common Matrix," NASA TN D-5532, Washington, D.C., Nov. 1969.
  40. L. G. Berry, ed., "X-ray Powder Data File," American Society for Testing Materials, Philadelphia, Penna., 1971.
  41. R. E. Vogel and C. P. Kempter, "A Mathematical Technique for the Precision Determination of Lattice Parameters," Acta. Cryst., vol. 14, 1961, 1130-1134.
  42. D. K. Smith, "A Revised Program for Calculating X-ray Powder Diffraction Patterns," UCRL-50264, Lawrence Radiation Laboratory, Livermore, Calif., 1967.
  43. E. E. Underwood, "Quantitative Metallography," Metals Engineering Quarterly, vol. 1, no. 3, 1961, 76.
  44. R. F. Decker and Wm. G. Wickersty, International Nickel Company, Inc., Sterling Forest, N.Y., Private communication, Nov. 1970.
  45. S. M. Sidik, "An Improved Multiple Linear Regression and Data Analysis Computer Package," NASA TN D-6770, 1972.
  46. Max Hansen and Kurt Anderko, "Constitution of Binary Alloys," 2nd ed., McGraw Hill Book Co., N.Y., 1958, p. 571.

47. Rodney P. Elliott, "Constitution of Binary Alloys, 1st Supplement," McGraw Hill Book Co., N.Y., 1965, p. 351.

TABLES

TABLE 1. - SUMMARY OF PHASES IN Ni-BASE SUPERALLOYS<sup>12</sup>

(a). Amount of gamma prime

Alloy	Amount gamma prime wt. %
B-1900	61.6
GMR 235	21.4
Inconel 700	25.9
Inconel 713C	50.0
Inconel X-750	14.5
IN 100	64.0
Mar-M200	55.8
Nicrotung	57.4
Nimonic 115	47.0
René 41	23.9
TRW 1900	63.3
Udimet 500	33.4
Udimet 700	35.4
Unitemp AF 1753	19.7
Waspaloy	22.1

TABLE 1. Continued. SUMMARY OF PHASES IN Ni-BASE SUPERALLOYS<sup>12</sup>

## (b). Composition of gamma phase

Alloy	Element, at. %, Ni is balance						
	Ti	Al	Cr	Co	Mo	W	Fe
B-1900	0.	5.1	18.3	16.1	5.4	-	-
GMR 235	.6	3.8	20.6	-	3.2	-	12.3
Inconel 700	1.0	4.0	19.4	32.2	2.4	-	.7
Inconel 713C	.1	8.1	24.3	-	3.9	-	-
Inconel X-750	1.2	.6	17.9	-	-	-	7.7
IN 100	.5	4.8	24.0	23.1	3.1	-	-
Mar-M200	0.	3.2	20.4	13.4	-	4.0	-
Nicrotung	1.0	.9	26.1	15.2	-	2.9	-
Nimonic 115	.6	4.6	26.5	19.7	2.9	-	-
René 41	.7	1.3	26.8	12.8	7.0	-	-
TRW 1900	.4	7.6	24.1	15.4	-	3.0	-
Udimet 500	.6	2.3	28.6	25.1	3.0	-	-
Udimet 700	1.5	5.3	24.3	23.5	3.9	-	-
Unitemp AF 1753	1.1	2.4	22.5	8.9	1.1	2.7	12.0
Waspaloy	.7	1.1	25.0	16.1	3.2	-	-

TABLE 1. - Concluded. SUMMARY OF PHASES IN Ni-BASE SUPERALLOYS<sup>12</sup>

(c). Composition of gamma prime phase

Alloy	Element, at. %, Ni is balance							
	Ti	Al	Cr	Co	Mo	W	Fe	Others
B-1900	1.9	17.2	3.0	5.8	2.3	-	-	1.9 Ta
GMR 235	5.1	17.6	2.3	-	1.4	-	2.7	
Inconel 700	6.7	13.6	4.3	11.9	1.2	-	-	
Inconel 713C	1.3	19.2	3.5	-	1.5	-	-	1.5 Nb
Inconel X-750	12.8	6.9	2.3	-	-	-	1.9	2.8 Nb
IN 100	8.6	14.0	3.4	9.7	.7	-	-	1.4 V
Mar-M200	3.7	14.8	3.1	7.5	-	4.0	-	1.1 Nb
Nicrotung	7.6	14.9	3.3	6.3	-	2.3	-	
Nimonic 115	7.2	15.7	4.1	7.5	.6	-	-	
René 41	10.9	9.2	3.5	2.3	1.3	-	-	
TRW 1900	1.4	17.4	3.9	6.5	-	2.6	-	1.2 Nb
Udimet 500	7.9	13.5	2.9	5.5	1.0	-	-	
Udimet 700	8.1	13.9	2.7	8.0	.9	-	-	
Unitemp AF 1753	11.6	11.6	1.3	2.8	.3	1.8	-	
Waspaloy	12.5	9.5	2.4	2.7	.7	-	-	

TABLE 2. - COMPOSITION OF ALLOYS

Heat	Composition, wt. %											
	Al		Cr		Mo		Ni		Ti		W	
	Aim	Anal.	Aim	Anal.	Aim	Anal.	Aim	Anal.	Aim	Anal.	Aim	Anal.
98	4.0	2.9	10.0	9.4	0.	0.	74.0	76.9	2.0	1.5	10.0	9.3
99	4.0	3.9	10.0	11.2	10.0	9.3	74.0	73.9	2.0	1.7	0.	0.
1	1.9	1.9	19.0	18.0	0.	0.	78.8	79.9	.2	.2	0.	0.
2	4.3	4.1	12.5	12.5	5.1	4.8	77.8	78.4	.2	.2	0.	0.
3	6.7	7.1	6.0	7.9	10.3	9.5	76.4	75.4	.2	.2	0.	0.
4	6.5	5.9	12.1	10.5	0.	0.	67.4	69.6	1.4	1.1	12.6	12.9
5	1.7	1.5	5.4	5.9	4.6	4.2	75.3	75.7	1.3	1.3	11.7	11.2
6	4.0	3.2	17.3	18.3	9.4	8.8	56.1	57.7	1.4	1.1	12.0	10.8
7	4.2	3.9	5.9	6.8	0.	0.	79.5	80.0	4.0	3.3	6.4	6.0
8	6.7	6.3	19.0	20.4	5.1	4.8	58.5	58.9	4.1	3.7	6.6	5.9
9	1.8	1.8	11.6	12.7	9.5	8.6	67.4	66.5	3.7	4.0	6.1	6.4
10	6.3	4.2	17.7	19.7	9.6	9.9	54.0	52.4	.2	.3	12.2	13.5
11	1.8	1.7	11.4	11.6	0.	0.	74.7	74.7	.2	.2	12.0	11.8
12	4.0	3.7	5.5	5.5	4.7	4.6	73.7	72.4	.2	.1	12.0	13.7
13	4.1	4.0	11.8	13.4	9.7	9.0	66.9	66.6	1.4	1.3	6.2	5.6
14	6.7	6.4	6.0	5.7	0.	0.	79.2	81.0	1.5	1.4	6.6	5.5
15	1.8	2.2	17.9	20.0	4.9	5.1	67.8	65.1	1.4	1.5	6.2	6.1
16	1.8	1.9	5.8	6.5	9.8	10.2	78.7	77.4	3.9	3.9	0.	0.
17	4.5	4.3	19.8	22.6	0.	0.	71.5	69.3	4.2	3.8	0.	0.
18	7.0	7.7	13.0	13.6	5.3	5.3	70.4	68.9	4.2	4.4	0.	0.
19	4.2	4.6	18.4	15.9	5.0	5.2	66.0	67.8	.2	.1	6.3	6.5
20	6.5	7.4	12.1	11.9	9.9	9.1	65.0	65.1	.2	.2	6.3	6.3
21	1.8	1.7	5.7	6.2	0.	0.	86.1	85.9	.2	.2	6.2	5.9
22	1.9	1.8	12.2	12.1	5.0	5.2	79.4	79.4	1.5	1.5	0.	0.
23	4.2	4.8	5.9	6.3	10.0	10.8	78.4	76.6	1.5	1.5	0.	0.
24	7.2	7.3	20.2	20.5	0.	0.	71.0	70.8	1.6	1.3	0.	0.
25	6.3	6.1	5.7	6.3	4.8	4.8	66.9	68.5	3.8	3.8	12.4	10.5
26	1.7	1.7	17.0	18.3	9.2	8.6	56.8	57.4	3.6	3.5	11.7	10.6
27	4.1	3.2	11.8	14.8	0.	0.	67.9	65.9	3.8	3.7	12.4	12.4
28	6.4	7.4	5.7	6.3	0.	0.	75.1	74.3	.2	.2	12.5	11.9
29	1.7	1.8	17.1	19.1	4.6	4.9	64.5	62.8	.2	.1	11.8	11.3
30	3.9	4.3	11.3	12.5	9.3	9.1	63.5	62.7	.2	.1	11.8	11.3
31	4.3	4.7	18.8	17.7	0.	0.	69.0	70.6	1.5	1.2	6.5	5.8
32	6.7	7.0	12.4	12.4	5.1	5.2	68.0	67.9	1.5	1.4	6.5	6.1
33	1.7	1.9	5.5	5.9	9.3	9.6	76.1	75.7	1.4	1.2	6.0	5.7
34	1.9	2.1	12.5	13.3	0.	0.	81.5	80.7	4.1	3.9	0.	0.
35	4.3	4.7	6.0	5.4	5.1	4.8	80.4	81.4	4.1	3.6	0.	0.
36	6.9	7.3	19.5	20.0	10.5	11.3	58.9	57.3	4.2	4.0	0.	0.
37	3.7	3.9	11.1	13.2	6.6	6.8	72.5	70.2	1.4	1.3	4.7	4.6
38	6.0	6.5	12.0	12.8	3.5	4.0	75.3	73.5	3.3	3.2	0.	0.
39	5.8	5.4	6.0	6.6	6.9	6.8	81.1	81.1	.2	.1	0.	0.
40	5.6	5.9	11.3	11.2	0.	0.	72.1	72.6	1.5	1.6	9.6	9.0
41	1.8	1.8	10.9	12.3	6.4	6.7	73.2	72.2	3.0	3.0	4.6	4.0
42	3.7	4.1	16.7	18.9	3.3	3.7	71.2	68.9	.2	.1	4.8	4.3
43	5.6	6.2	11.3	11.5	6.7	7.0	71.3	70.9	.2	.2	4.8	4.2
44	5.5	5.0	5.8	5.7	3.3	3.3	72.9	74.3	3.1	2.7	9.4	8.9
45	1.8	1.6	15.8	16.8	6.3	6.5	64.2	64.3	2.9	3.1	9.0	7.8
46	3.6	4.1	10.7	10.9	6.3	7.9	70.1	68.6	.2	.3	9.1	8.2
47	5.7	5.6	11.5	11.5	3.4	3.5	73.0	73.2	1.5	1.3	4.9	4.8
48	4.0	3.6	17.7	17.5	0.	0.	75.1	75.2	3.3	3.8	0.	0.
49	6.1	5.5	18.0	17.2	0.	0.	74.4	75.6	1.6	1.7	0.	0.

TABLE 3. - EXPERIMENTAL DESIGN

Element	Level	Alloying addition, at. %, Ni is balance Heat Number	
		1-36	37-49
Al	Low	4.0	4.0
	Medium	9.0	8.0
	High	13.0	12.0
Ti	Low	0.25	0.25
	Medium	1.75	1.75
	High	4.75	3.75
Cr	Low	6.5	6.5
	Medium	13.5	12.5
	High	20.5	18.5
W	Low	0	0
	Medium	2.0	1.5
	High	4.0	3.0
Mo	Low	0	0
	Medium	3.0	2.0
	High	6.0	4.0

TABLE 4. - RAW MATERIALS

Element	Form	Purity, wt. %
Aluminum	Granulated ingot	99.8
Chromium	Electrolytic	99.8
Molybdenum	Chips	99.5
Nickel	Electrolytic	99.9
Titanium	Sponge	99.3
Tungsten	Powder	99.95

TABLE 5. - COMPARISON OF CHEMICAL ANALYSIS

Heat	Element					wt. %	Lab.
	Al	Cr	Mo	Ti	W		
2	4.3	13.3	4.8	0.2	---	a <sub>1</sub> b <sub>2</sub> c Aim	
	4.1	12.5	4.8	.2	---		
	4.3	12.5	5.1	.2	---		
12	3.9	5.5	4.2	0.2	11.8	1 2 Aim	
	3.7	5.5	4.6	.1	13.7		
	4.0	5.5	4.7	.2	12.0		
14	7.4	6.2	-	1.5	6.4	1 2 Aim	
	6.4	5.7	-	1.4	5.5		
	6.7	6.0	-	1.5	6.6		
15	1.9	18.9	4.7	1.2	6.5	1 2 Aim	
	2.2	20.0	5.1	1.5	6.1		
	1.8	17.9	4.9	1.4	6.2		
16	1.8	6.0	9.3	3.6	---	1 2 Aim	
	1.9	6.5	10.2	3.9	---		
	1.8	5.8	9.8	3.9	---		
19	4.4	15.1	4.9	0.1	6.8	1 2 Aim	
	4.6	15.9	5.2	.1	6.5		
	4.2	18.4	5.0	.2	6.3		
22	1.9	11.7	4.8	1.4	---	1 2 Aim	
	1.8	12.1	5.2	1.5	---		
	1.9	12.2	5.0	1.5	---		
23	4.5	5.9	9.4	1.4	---	1 2 Aim	
	4.8	6.3	10.8	1.5	---		
	4.2	5.9	10.0	1.5	---		
28	8.0	5.7	-	0.1	12.2	1 2 Aim	
	7.4	6.3	-	.2	11.9		
	6.4	5.7	-	.2	11.8		
34	2.4	12.4	-	4.1	---	1 2 Aim	
	2.1	13.3	-	3.9	---		
	1.9	12.5	-	4.1	---		
35	4.5	5.9	5.0	4.1	---	1 2 Aim	
	4.7	5.4	4.8	3.6	---		
	4.3	6.0	5.1	4.1	---		

## TABLE 5. - Concluded. COMPARISON OF CHEMICAL ANALYSIS

<sup>a</sup>Lab 1 is an independent chemical laboratory.

<sup>b</sup>Lab 2 used only spectrographic analysis. The technique is the same as was used to analyze the extracted residues.

<sup>c</sup>AIM is the charge ratio of elements. No attempt was made to compensate for melting losses.

TABLE 6. - MULTIPHASE ALLOYS

AMOUNT OF VARIOUS RESIDUES PRODUCED WITH TWO ELECTROLYTES

Heat	Yield, wt. %, electrolyte		Phases
	HCl	(NH <sub>4</sub> ) <sub>2</sub> SO <sub>4</sub>	
3	1.7		mu
4	7.6		<sup>a</sup> W
6	12.0		W, sigma
8	11.0		Cr, W, sigma
9	0.8		mu, W
10	12.0		W, sigma
13	6.4		mu
17	.6	19.6	Cr
18	14.3		Cr, sigma
19	0.06	37.0	mu, W
20	14.5		sigma, W
24	.9	8.6	Cr, 1 line 2.21
25	9.5		sigma, W
26	15.0		sigma, mu, W
27	4.5		W, Cr
29	.4	5.0	W
30	7.1		W, mu
32	14.2		Cr, W, sigma
36	19.4		Cr, W, sigma
43	1.0	52.8	mu
44	0.9	30.3	unidentified
45	3.7	28.7	mu, W

<sup>a</sup>W and Mo solid solutions cannot be differentiated by X-ray diffraction. W is used to identify a bcc phase with an A<sub>0</sub> near that of W or Mo.

TABLE 7 - SUMMARY OF X-RAY DIFFRACTION DATA OF GAMMA AND GAMMA PRIME

Heat	$\frac{I(100)}{I(200)}$ $\gamma'$		Lattice parameter, $A_0$ $10^{-10} \text{ M } (\text{Å})$		Density, g/cc	
	Obs.	Calc.	$\gamma'$	$\gamma$	$\gamma'$	$\gamma$
98	1.5	1.1	3.582	3.566	8.4	8.9
99	7.2	13.5	3.580	3.582	7.9	8.5
2	7.4	17.4	3.570	3.566	7.9	8.4
5				3.574		
7	nil	5.4	3.578	3.557	8.2	8.6
12	nil	.3	3.576	3.574	8.6	9.3
14	3.1	2.2	3.570	3.571	8.4	8.1
15	3.2	3.5	3.583	3.589	8.2	8.5
16	3.4	10.7	3.587	3.587	7.9	8.6
17	5.5		3.580	3.580		
19	1.8		3.576	3.588		
21				3.548		
22	3.8	6.8	3.577	3.565	8.1	8.5
23	3.9	12.7	3.577	3.579	7.9	8.6
24	15.2		3.576	3.570		
28	nil	.8	3.574	3.574	9.6	8.2
29	nil		3.577	3.590		
31	nil	6.3	3.578	3.579	8.1	8.2
34	8.3	17.2	3.584	3.556	7.8	8.3
35	5.4	10.5	3.579	3.578	7.9	8.3
37	nil	6.5	3.578	3.585	8.1	8.6
38	7.3	16.0	3.578	3.578	7.8	7.9
39	6.3	9.5	3.571	3.570	8.0	8.3
40	nil	2.7	3.577	3.576	8.4	8.2
41	nil	1.0	3.586	3.579	8.5	8.6
42	nil	4.3	3.575	3.579	8.2	8.3
43	3.0		3.579	3.581		
44	nil		3.580	3.588		
45	nil		3.588	3.595		
46	1.4	.9	3.581	3.582	8.5	8.8
47	3.2	5.3	3.578	3.578	8.2	8.2
48	5.2	17.0	3.578	3.568	7.8	8.1
49	6.7	17.8	3.570	3.570	7.8	7.9

TABLE 8. - EXTRACTION SUMMARY FOR TWO PHASE ALLOYS

Heat	Extraction yield, wt. %	
	HCl	gamma prime
98	0.1	40.1
99	.5	39.4
2	nil	29.3
5	.1	25.6
7	nil	39.2
12	nil	31.9
14	.4	18.4
15	nil	16.8
16		20.3
21	↓	.4
22		8.5
23		44.5
28		32.1
31		41.3
33		21.4
34		21.5
35	↓	54.5
37	.06	35.3
38	nil	34.2
39		44.7
40	↓	55.7
41	.05	23.9
42	nil	27.1
46	.04	29.3
47	.07	55.6
48	.06	38.7
49	nil	51.9

<sup>a</sup>Electrolyte was  $H_3PO_4$ .

TABLE 9. - COMPOSITION OF GAMMA PRIME

Heat	Element, at. %					
	Ni	Al	Cr	Mo	Ti	W
98	78.0	12.5	2.7	-	3.7	3.1
99	76.1	13.8	2.6	2.9	3.9	-
2	74.5	17.3	5.1	2.4	.7	-
5	75.7	13.3	2.1	1.1	5.1	2.7
7	76.9	11.7	2.4	-	7.1	1.9
12	77.8	14.6	1.9	1.5	.3	3.9
14	73.3	15.9	4.2	-	2.8	3.8
15	74.3	11.3	4.9	1.1	6.3	2.1
16	75.6	10.3	1.5	2.3	10.3	-
22	76.2	7.8	8.9	2.2	4.9	-
23	74.2	15.9	2.7	3.9	3.3	-
28	72.1	16.9	3.5	-	.3	7.2
31	74.3	16.0	4.0	-	3.3	2.4
33	77.1	10.8	2.4	2.4	5.9	1.4
34	73.1	10.1	2.9	-	13.9	-
35	77.3	12.1	2.3	1.7	6.6	-
37	74.7	15.7	2.7	1.7	3.5	1.7
38	74.7	15.1	3.5	1.6	5.1	-
39	77.5	15.5	3.2	3.5	.3	-
40	76.0	15.1	3.3	-	2.3	3.3
41	72.4	10.6	2.1	2.9	9.5	2.5
42	73.6	17.5	4.6	1.3	.3	2.7
46	76.6	14.9	2.9	1.7	.4	3.5
47	75.8	15.3	3.2	1.3	2.4	2.0
48	76.1	13.1	3.9	-	6.9	-
49	75.9	15.3	2.7	-	2.7	-
S		0.851	0.336	0.573	0.502	0.852

TABLE 10. - COMPARISON OF AMOUNT OF GAMMA PRIME IN ALLOYS

Heat	Observed		Calculated vol. %
	vol. %	wt. %	
98	52	40	41
99	43	39	41
2	24	29	30
15	13	17	17
21	4	.5	<sup>a</sup> na
23	55, 58	45	50
29	7	5	<sup>a</sup> na
31	45	41	41
33	8	1 (H <sub>3</sub> PO <sub>4</sub> )	<sup>a</sup> na
34	20	21	22
39	50	45	46

<sup>a</sup>na, not available because density of  $\gamma$  could not be determined.

TABLE 11. - COMPARISON OF OBSERVED AND CALCULATED DENSITIES

Heat	Density, g/cc	
	Calculated	Observed
98	8.7	8.6
99	8.3	8.2
2	8.2	8.1
7	8.4	8.5
14	8.2	8.2
15	8.5	8.5
16	8.4	8.4
22	8.5	8.4
23	8.3	8.3
28	8.6	8.5
31	8.2	8.2
34	8.2	8.2
35	8.1	8.1
37	8.4	8.4
38	7.9	7.9
39	8.2	8.2
40	8.3	8.4
41	8.6	8.6
42	8.3	8.3
46	8.7	8.7
47	8.2	8.2
48	8.0	7.9
49	7.8	7.9

TABLE 12. - COMPOSITION OF GAMMA

Heat	Element, at. %, balance is Ni				
	Al	Cr	Mo	Ti	W
98	2.1	16.4	-	.5	2.9
99	4.3	19.1	7.5	.8	-
2	4.7	17.2	3.0	0.	-
7	6.1	10.9	-	1.7	1.9
12	5.5	8.9	3.7	.1	5.0
14	12.7	6.6	-	1.5	1.2
15	3.5	26.5	3.6	.9	1.9
16	2.1	9.2	7.5	3.1	-
22	3.4	13.9	3.2	1.5	-
23	5.1	10.7	8.7	.5	-
28	15.4	8.5	-	.1	2.2
31	5.5	29.9	-	.1	1.3
34	2.5	17.7	-	1.9	-
35	6.9	10.3	4.2	1.2	-
37	4.3	21.8	5.5	.5	1.3
38	11.9	18.5	2.7	2.9	-
39	7.6	10.5	4.3	0.	-
40	9.5	23.3	-	1.5	2.1
41	1.9	17.8	4.5	1.9	.9
42	5.5	25.7	2.5	.1	.8
46	6.7	16.7	6.3	.4	2.3
47	7.5	24.4	3.1	.5	.8
48	3.5	27.7	-	2.5	-
49	6.2	30.7	-	1.1	-
S	0.640	0.391	0.224	0.256	0.374

TABLE 13. - REGRESSION ANALYSIS OF GAMMA AND GAMMA PRIME

n	Phase		factor, F <sub>n</sub>
	γ coefficient, B <sub>n</sub>	γ' coefficient, B <sub>n</sub>	
0	13.3992	7.42647	constant
1	-1.07392	3.59713	Cr
2	1.80069	0.0	Mo
3	0.0	.849058	Ti
4	15.3168	-.589230	W
5	.0318507	-.292157	Cr <sup>2</sup>
6	-.0455815	.149930	Mo <sup>2</sup>
7	1.53473	-.0256415	Ti <sup>2</sup>
8	-2.59870	-.0398181	W <sup>2</sup>
9	-.100793	-.127831	Cr x Mo
10	-.204796	-.310730	Cr x Ti
11	-.504191	.290021	Cr x W
12	-2.12721	-.245979	Mo x Ti
13	.598921	.876515	Mo x W
14	-7.75600	-.155343	Ti x W
15	.153165	.0675603	Cr x Mo x Ti
16	0.0	-.275617	Cr x Mo x W
17	.486625	0.0	Cr x Ti x W
18	-1.43936	.0226054	Mo x Ti x W
R <sup>2</sup>	.89	.87	

$$\text{Equation: } A_1 = \sum_{n=0}^{n=18} B_n \times F_n$$

TABLE 14. - LEAST SQUARES ANALYSIS OF DIRECTION NUMBERS

n	Element				
	Al	Mo	Ti	W	
	coefficient, $B_n$	coefficient, $B_n$	coefficient, $B_n$	coefficient, $B_n$	factor, $F_n$
0	-2.4316	-.0032572	-1.04691	-.52841	constant
1	.066096	-.0010339	.046595	-.054240	Al
2	.059819	-.013136	.030941	.030041	Cr
3	.0088685	.087981	.026712	.020858	Mo
4	.14622	.021598	-.070565	.054511	Ti
5	.090661	.024404	.040548	.14031	W
$R^2$	.64	.72	.76	.37	
$T^a$	.35	.09	.96	.29	

$$\text{Equation: Direction Number} = \sum_{n=0}^{n=5} B_n \times F_n$$

<sup>a</sup>T is the significance level of the least significant coefficient.

TABLE 15. - COMPARISON OF OBSERVED AND ESTIMATED  
PHASE COMPOSITIONS IN EXPERIMENTAL ALLOYS

heat	phase	element, At. %									
		Al		Cr		Mo		Ti		W	
		a <sub>obs</sub>	b <sub>est</sub>	obs	est	obs	est	obs	est	obs	est
98	γ	2.1	4.1	16.4	13.6	-	-	0.5	0.6	2.9	2.9
	γ'	12.5	12.7	2.7	3.2	-	-	3.7	5.0	3.1	3.2
99	γ	4.3	4.3	19.1	17.1	7.5	7.2	0.8	0.7	-	-
	γ'	13.8	14.8	2.6	4.0	2.9	2.5	3.9	4.5	-	-
2	γ	4.7	3.9	17.2	18.1	3.0	3.1	0.0	0.0	-	-
	γ'	17.3	12.9	5.1	9.1	2.4	2.5	0.7	1.0	-	-
5	γ	<sup>c</sup> NA	0.8	NA	9.6	NA	3.5	NA	0.4	NA	4.2
	γ'	13.3	10.7	2.1	1.0	3.1	1.1	5.1	5.1	2.7	2.7
7	γ	6.1	8.0	10.9	7.9	-	-	1.7	3.6	1.9	1.8
	γ'	11.7	11.3	2.4	3.1	-	-	7.1	6.6	1.9	3.1
12	γ	5.5	8.6	8.9	6.6	3.7	3.0	0.1	0.2	5.9	4.6
	γ'	14.6	13.6	1.9	1.5	1.5	1.6	0.3	1.2	3.9	5.0
14	γ	12.7	4.4	6.6	17.4	-	-	1.5	0.0	1.2	0.0
	γ'	15.9	15.3	4.2	3.5	-	-	2.8	2.5	3.8	3.7
15	γ	3.5	4.8	26.5	22.7	3.6	3.1	0.9	1.9	1.9	2.0
	γ'	11.3	8.3	4.9	9.9	1.1	2.4	6.3	3.1	2.1	0.0
16	γ	2.1	1.7	9.2	9.8	7.5	7.7	3.1	2.8	-	-
	γ'	10.3	9.9	1.5	1.3	2.3	3.0	10.3	9.6	-	-
22	γ	3.4	3.4	13.9	13.9	3.2	3.2	1.5	1.6	-	-
	γ'	7.8	7.6	8.9	10.0	2.2	2.7	4.9	3.5	-	-
23	γ	5.1	5.6	10.7	11.4	8.7	8.6	0.5	0.4	-	-
	γ'	15.9	14.8	2.7	2.5	3.9	4.2	3.3	3.2	-	-
28	γ	15.4	13.7	8.5	10.4	-	-	0.1	0.2	2.2	1.5
	γ'	16.9	17.8	3.5	3.7	-	-	0.3	0.2	7.2	5.9
31	γ	5.5	6.6	29.9	12.1	-	-	0.1	1.1	1.3	2.4
	γ'	16.0	15.9	4.0	3.7	-	-	3.3	2.1	2.4	4.4
33	γ	NA	2.4	NA	8.4	NA	6.8	NA	0.9	NA	1.8
	γ'	10.8	12.5	2.4	0.5	2.4	2.7	5.9	4.9	1.4	2.3
34	γ	2.5	1.6	17.7	18.6	-	-	1.9	1.4	-	-
	γ'	10.1	12.0	2.9	1.9	-	-	13.9	13.7	-	-
35	γ	6.9	5.3	10.3	11.4	4.2	4.2	1.2	0.6	-	-
	γ'	12.1	12.7	2.3	2.2	1.7	1.9	6.6	6.5	-	-

TABLE 15. - Concluded. COMPARISON OF OBSERVED AND ESTIMATED  
PHASE COMPOSITIONS IN EXPERIMENTAL ALLOYS

heat	phase	element, At. %									
		Al		Cr		Mo		Ti		W	
		<sup>a</sup> obs	<sup>b</sup> est	obs	est	obs	est	obs	est	obs	est
37	Y	4.3	5.3	21.8	20.0	5.5	5.3	0.5	0.9	1.3	0.7
	Y'	15.7	15.0	3.5	4.5	1.6	1.5	5.1	5.5	-	-
38	Y	11.9	12.7	18.9	14.7	2.7	2.4	2.9	3.3	-	-
	Y'	15.1	15.0	3.5	4.5	1.6	1.5	5.1	5.5	-	-
39	Y	7.6	10.5	10.5	7.6	4.3	4.1	0.0	0.0	-	-
	Y'	15.5	15.9	3.2	3.2	3.5	3.0	0.3	0.9	-	-
40	Y	9.5	7.1	23.3	28.2	-	-	1.5	0.2	2.1	0.0
	Y'	15.1	15.3	3.3	4.0	-	-	2.3	2.8	3.3	5.6
41	Y	1.9	0.5	17.8	19.6	4.5	5.7	1.9	0.8	0.9	2.1
	Y'	10.6	8.0	2.1	7.6	2.9	2.3	9.5	7.0	2.5	0.4
42	Y	5.5	6.2	25.7	26.3	2.5	2.2	0.1	0.2	0.8	0.5
	Y'	17.5	15.6	4.6	5.4	1.3	2.2	0.3	0.2	2.7	3.4
46	Y	6.7	9.2	16.7	12.5	6.3	4.9	0.4	0.4	2.3	2.7
	Y'	14.9	14.4	2.9	5.3	1.3	1.6	2.4	2.2	2.0	4.9
47	Y	7.5	5.8	24.4	23.9	3.1	2.9	0.5	0.4	0.8	1.3
	Y'	15.3	15.7	3.2	5.1	1.3	1.6	2.4	2.2	2.0	4.9
48	Y	3.5	5.3	27.7	27.6	-	-	2.5	0.6	-	-
	Y'	13.1	10.5	3.9	3.7	-	-	6.9	10.8	-	-
49	Y	6.2	6.7	30.7	29.5	-	-	1.1	0.5	-	-
	Y'	15.3	15.6	2.7	5.1	-	-	2.7	3.4	-	-

<sup>a</sup>obs is the experimentally observed value.

<sup>b</sup>est is the value estimated by the calculation.

<sup>c</sup>NA not available.

TABLE 16. - REGRESSION ANALYSIS OF GAMMA AND GAMMA PRIME  
LATTICE PARAMETERS

element	coefficient, $A_0/\text{at. } \%$		
	$\gamma$		$\gamma'$
	current work	<sup>b</sup> reference: 4	current work
Al	.00106	.00186	-.000736
Cr	.000753	.00105	-.000910
Mo	.00261	.00435	.000508
Ti	<sup>a</sup> -.000597	.00337	.000518
W	.00215	.00412	.000490
Nb	-	.00645	-
Fe	-	.00115	-
constant	3.545	3.5240	3.587
$R^2$	.75	-	.66
$\sigma$	.0043	-	.0026

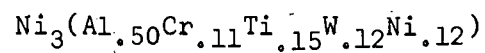
<sup>a</sup>The coefficient for Ti in  $\gamma$  is not significant at .51, but all others in this study are significant at .84.

<sup>b</sup>Reference 4 uses the same coefficients for  $\gamma'$ , but the constant is 3.5208.

TABLE 17. - DEGREE OF LONG RANGE ORDER IN GAMMA PRIME

heat	<sup>a</sup> formula									<sup>b</sup> <sub>S</sub>
	(Ni	Cr)	3	(Al	Cr	Ti	Mo	W	Ni)	
98	1.0	-		.50	.11	.15	-	.12	.12	1.0
99	1.0	-		.55	.11	.16	.12	-	.05	.73
2	.99	.01		.68	.20	.03	.09	-	-	.65
14	.98	.02		.64	.10	.11	-	.15	-	1.0
15	.99	.01		.45	.17	.26	.04	.08	-	.96
16	1.0	-		.41	.06	.41	.10	-	.02	.56
22	1.0	-		.32	.36	.20	.08	-	.04	.75
23	.99	.01		.63	.08	.13	.16	-	-	.55
34	.97	.03		.40	.04	.56	-	-	-	.69
35	1.0	-		.49	.09	.26	.07	-	.09	.72
38	.99	.01		.61	.12	.20	.07	-	-	.68
39	1.0	-		.62	.13	.01	.14	-	.10	.81
46	1.0	-		.60	.12	.02	.07	.13	.06	1.0
47	1.0	-		.61	.13	.10	.05	.08	.03	.78
48	1.0	-		.52	.16	.28	-	-	.04	.55
49	1.0	-		.61	.24	.11	-	-	.04	.61

<sup>a</sup>Formula assumed for perfect order (S 1.0). Example heat 98



<sup>b</sup><sub>S</sub> is the long range order parameter.

TABLE 18. - OCCURRENCE OF PHASES

Alloy	Element, At. %						Phase			
	Al	Cr	Mo	Ti	W	Ni	Cr	<sup>a</sup> Mo,W	$\sigma$	$\mu$
3	14.6	8.4	5.5	.2	-	71.2				X
4	12.9	11.9	-	1.3	4.1	69.8		X		
6	7.3	21.6	5.6	1.4	3.6	60.5		X	X	
8	13.1	21.9	2.8	4.3	1.8	56.1	X	X	X	
9	4.0	14.8	5.4	5.1	2.1	68.6		X		X
10	9.7	23.5	6.4	.4	4.6	55.4		X	X	
13	8.8	15.2	5.5	1.6	1.8	67.1				X
17	8.6	23.4	-	4.3	-	63.7	X			
18	15.3	14.0	3.0	4.9	-	62.9	X		X	
19	9.9	17.8	3.1	.1	2.1	67.0		X		X
20	15.7	13.1	5.4	.2	2.0	63.5		X	X	
24	14.2	20.7	-	1.4	-	63.6	X			
25	13.3	7.1	2.9	4.6	3.4	68.6		X	X	
26	3.9	21.8	5.6	4.5	3.6	60.6		X	X	X
27	7.1	17.0	-	4.6	4.0	67.2	X	X		
29	4.1	22.7	3.2	.1	3.8	66.1		X		
30	9.8	14.8	5.8	.1	3.8	65.7		X		X
32	14.7	13.7	3.1	1.7	1.9	65.3	X	X	X	
36	14.8	21.0	6.4	4.5	-	55.3	X	X	X	
43	12.9	12.5	4.1	4.9	1.3	64.2				X
44	10.9	6.4	2.0	3.3	2.9	74.5		unidentified		
45	3.6	19.6	4.1	3.9	2.6	66.2		X		X

<sup>a</sup>Mo and W cannot be differentiated by X-ray diffraction. BCC Phase with  $A_0$  at a approximately  $3.15 \text{ \AA}$ .

TABLE 19. - COMPOSITION OF HCl EXTRACTION RESIDUES

heat	phase	element, at. %						
		Al	Cr	Mo	Ni	Ti	W	Zr
9	$\mu, W$	0.	18.4	33.7	36.4	5.9	5.6	0.
13	$\mu$	0.	23.3	35.7	34.8	.3	5.8	0.
17	Cr	0.	91.2	0.	2.7	4.2	0.	1.9
24	Cr	0.	94.3	0.	1.7	3.9	0.	.1
43	$\mu$	2.3	23.5	22.9	43.2	0.	5.1	2.9
44	<sup>a</sup> X	1.4	15.0	25.6	29.4	2.9	25.8	0.
45	$\mu, W$	.3	26.6	21.4	33.7	1.8	16.1	0.

<sup>a</sup>The X-ray diffraction pattern could not be identified.

TABLE 20. - COMPOSITION OF COMMERCIAL SUPERALLOYS

	Heat treatment	Weight percent (balance is nickel)										
		Cr	Co	Al	Ti	W	Mo	Nb	Ta	V	Fe	C
B-1900	1	7.9	9.8	5.9	1.0	--	5.7	-	4.5	-	-	0.09
GMR 235	1	15.9	--	3.5	2.0	--	5.0	-	-	-	9.8	.15
Inconel 700	2	14.3	28.5	3.0	2.5	--	3.9	-	-	-	.7	.12
Alloy 713C	1	12.6	--	<sup>a</sup> 6.8	.8	--	4.7	2.1	-	-	-	.16
Inconel X-750	3	14.6	--	.8	2.4	--	-	.8	-	-	6.5	.04
IN 100	1	9.8	15.0	5.6	<sup>a</sup> 5.7	--	3.1	-	-	0.9	-	.19
Mar-M 200	1	8.9	9.5	4.5	1.9	12.3	-	1.1	-	-	-	.16
Nicrotung	1	11.0	9.9	4.4	4.2	8.0	-	-	-	-	-	.07
Nimonic 115	4	14.8	14.8	4.8	3.9	--	3.5	-	-	-	-	.14
René 41	5	19.0	10.7	1.5	3.1	--	9.7	-	-	-	-	.09
TRW 1900	1	10.1	10.3	6.7	1.0	9.2	-	1.6	-	-	-	.14
Udimet 500	6	18.7	19.3	2.9	3.0	--	4.3	-	-	-	-	.07
Udimet 700	7	15.4	18.8	4.4	3.4	--	5.0	-	-	-	-	.06
Unitemp AF 1753	8	16.4	7.7	2.0	3.4	8.3	1.5	-	-	-	9.0	.23
Waspaloy	9	18.6	13.0	1.4	2.9	--	4.2	-	-	-	-	.05

<sup>a</sup>Value higher than AMS specification for alloy.

Heat treatment	Description
1	As cast
2	1180° C/ 2 hr/air cool + 870° C/ 4 hr/air cool
3	1150° C/ 2 hr/air cool + 843° C/ 24 hr/air cool + 704° C/ 20 hr/air cool
4	1190° C/ 1 1/2 hr/air cool + 1100° C/ 6 hr/air cool
5	1060° C/ 4 hr/air cool + 760° C/ 16 hr/air cool
6	1080° C/ 4 hr/air cool + 843° C/ 24 hr/air cool + 760° C/ 16 hr/air cool
7	1170° C/ 4 hr/air cool + 1032° C/ 136 hr/air cool
8	1170° C/ 4 hr/air cool + 899° C/ 6 hr/air cool
9	1080° C/ 4 hr/air cool + 843° C/ 24 hr/air cool + 760° C/ 16 hr/air cool

TABLE 21. - COMPARISON OF OBSERVED AND ESTIMATED PHASE  
COMPOSITIONS IN COMMERCIAL ALLOYS

alloy	phase	element, at. %									
		Al		Cr		Mo		Ti		W	
		<sup>a</sup> obs	<sup>b</sup> est	obs	est	obs	est	obs	est	obs	est
B-1900	Y	5.1	1.8	18.3	20.5	5.4	5.7	0.	0.	-	-
	Y'	17.2	16.4	3.0	4.4	2.3	2.6	1.9	1.7	-	-
GMR 235	Y	3.8	3.5	20.6	22.5	3.2	3.3	0.6	0.4	-	-
	Y'	17.6	14.3	2.3	6.0	1.4	2.2	5.1	4.4	-	-
Inconel 700	Y	4.0	4.8	19.4	16.9	2.4	2.3	1.0	1.7	-	-
	Y'	13.6	13.0	4.3	5.7	1.2	1.8	6.7	6.4	-	-
Inconel 713C	Y	8.1	5.4	24.3	27.2	3.9	3.6	0.1	0.6	-	-
	Y'	19.2	18.0	3.5	6.5	1.5	2.3	1.3	0.6	-	-
Inconel X-750	Y	0.6	0.5	17.9	16.9	-	-	1.2	2.0	-	-
	Y'	6.9	15.5	2.3	1.5	-	-	12.8	12.5	-	-
IN 100	Y	4.8	10.4	24.0	14.8	3.1	2.4	0.5	3.0	-	-
	Y'	14.0	13.4	3.4	1.2	0.7	0.6	8.6	10.7	-	-
Mar M 200	Y	3.2	0.5	20.4	29.4	-	-	0.	0.	4.2	2.1
	Y'	14.8	13.5	3.1	3.4	-	-	3.7	3.6	4.0	4.9
Nicrotung	Y	0.9	8.4	26.1	18.3	-	-	1.0	1.8	2.9	2.1
	Y'	14.9	10.6	3.3	4.9	-	-	7.6	8.2	2.3	3.0
Nimonic 115	Y	4.6	8.8	26.5	19.1	2.9	2.1	0.6	2.6	-	-
	Y'	15.7	12.8	4.1	3.6	0.6	1.4	7.2	8.4	-	-
René 41	Y	1.3	0.5	26.8	27.6	7.0	8.2	0.7	1.1	-	-
	Y'	9.2	9.3	3.5	5.3	1.3	1.0	10.9	9.2	-	-
TRW 1900	Y	7.6	7.4	24.1	27.3	-	-	0.4	0.9	3.0	1.8
	Y'	17.4	17.5	3.9	3.9	-	-	1.4	0.9	2.6	6.6
Udimet 500	Y	2.3	3.7	28.6	26.7	3.0	2.6	0.6	1.0	-	-
	Y'	13.5	10.7	2.9	5.6	1.0	2.1	7.9	8.3	-	-
Udimet 700	Y	5.3	6.8	24.3	24.0	3.9	3.8	1.5	1.3	-	-
	Y'	13.9	12.5	2.7	4.0	0.9	1.5	8.1	7.6	-	-
Unitemp AF 1753	Y	2.4	4.4	22.5	18.1	1.1	0.9	1.1	2.7	2.7	3.4
	Y'	11.6	7.9	1.3	8.0	0.3	0.9	11.6	5.9	1.8	0.
Waspaloy	Y	1.1	0.5	25.0	24.6	3.2	2.6	0.7	1.2	-	-
	Y'	9.5	11.2	2.4	4.3	0.7	2.1	12.5	10.6	-	-

<sup>a</sup>obs is the experimentally observed value (ref. 12).

<sup>b</sup>est is the value estimated by the calculation.

TABLE 22. - PHASE OCCURRENCE IN COMMERCIAL ALLOYS

Alloy	Parameters			<sup>c</sup> Phase
	<sup>a</sup> Alloy Ni+Co+Fe at. %	<sup>a</sup> Gamma Cr + 1.75 x (Mo+W) at. %	<sup>b</sup> Al DN GT -0.3	
Inconel X-750	78.9	17.9		<sup>d</sup> <sub>n</sub>
Mar M 200	73.1	27.4		n
Inconel 700	72.6	23.6		n
B-1900	72.5	27.0		n
Nicrotung	70.7	31.2	X	n
Waspaloy	70.5	30.6		n
GMR 235	69.9	26.2		-
TRW 1900	69.1	29.4		n
IN 100	<sup>e</sup> 68.7	29.4	X	sigma
Unitemp AF 1753	68.4	29.2		n
Nimonic 115	67.7	31.6	X	sigma
Udimet 500	67.6	33.9		↓
Udimet 700	67.5	31.1	X	
Inconel 713C	<sup>e</sup> 67.5	31.1		
René 41	65.6	39.1		.mu

<sup>a</sup>Compositions from reference 12.

<sup>b</sup>Al direction number calculated using composition in reference 12 and computer program from the Appendix.

<sup>c</sup>Phases were taken from reference 16.

<sup>d</sup><sub>n</sub> - no sigma or mu was reported.

<sup>e</sup>Composition did not meet AMS specification for alloy.

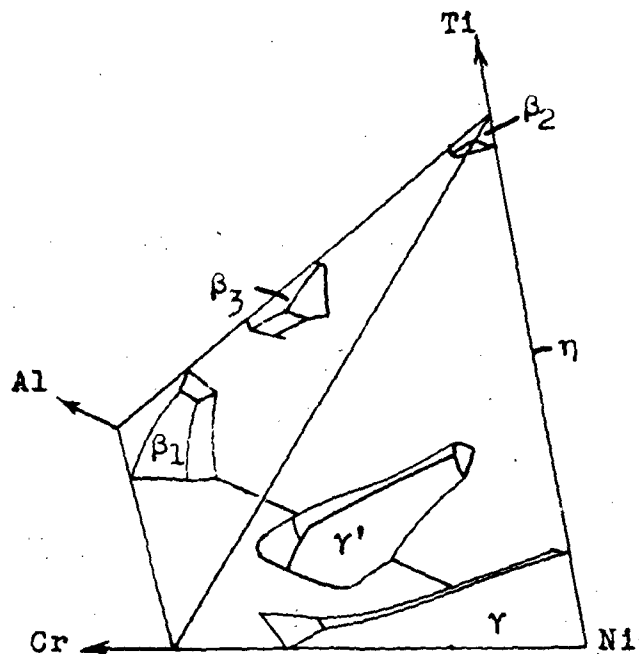
TABLE 23. - LATTICE PARAMETER OF GAMMA PRIME IN COMMERCIAL ALLOYS

Alloy	Parameter, A°	
	<sup>a</sup> observed	<sup>b</sup> estimated
GMR 235	3.580	3.582
Inconel 700	3.582	3.581
Inconel 713C	3.581	3.581
Inconel X-750	3.598	3.599
Mar M 200	3.582	3.589
Nicrotung	3.591	3.588
TRW 1900	3.581	3.582
Udimet 500	3.584	3.581
Udimet 700	3.582	3.582
Unitemp AF 1753	3.590	3.592
Waspaloy	3.590	3.587

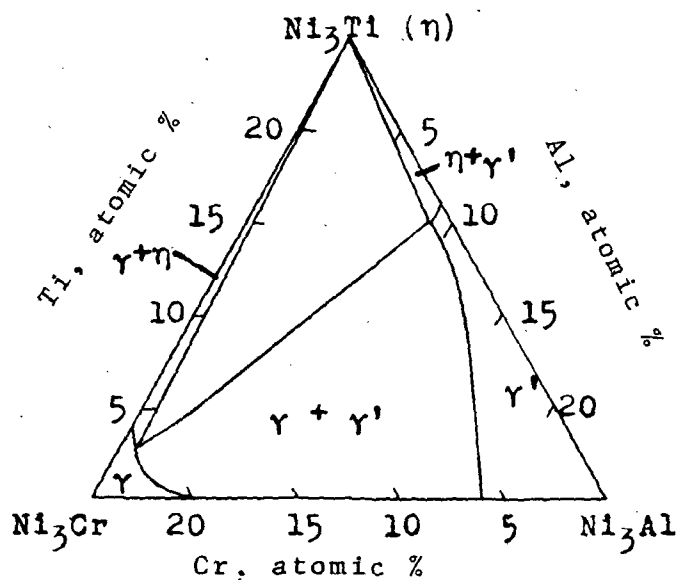
<sup>a</sup>Reference 12.

<sup>b</sup>Coefficients from Table 16 and reference 4.

FIGURES



(a) Quaternary section showing 1 phase fields



(b) Pseudo-ternary section at 75% Ni

FIGURE 1 Ni-RICH REGION OF Ni-Al-Cr-Ti SYSTEM AT 750°C (ref.3)

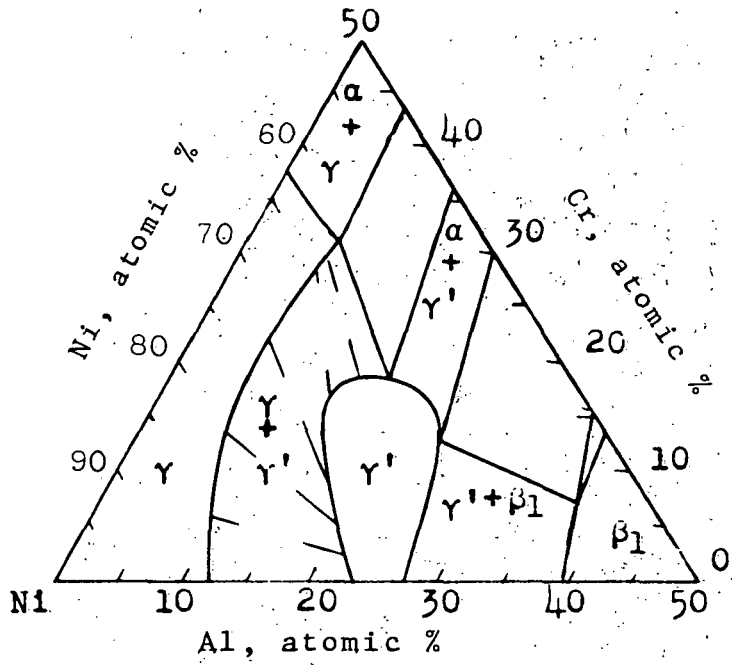


FIGURE 2 Ni-Al-Cr SYSTEM AT 750°C (ref.6)

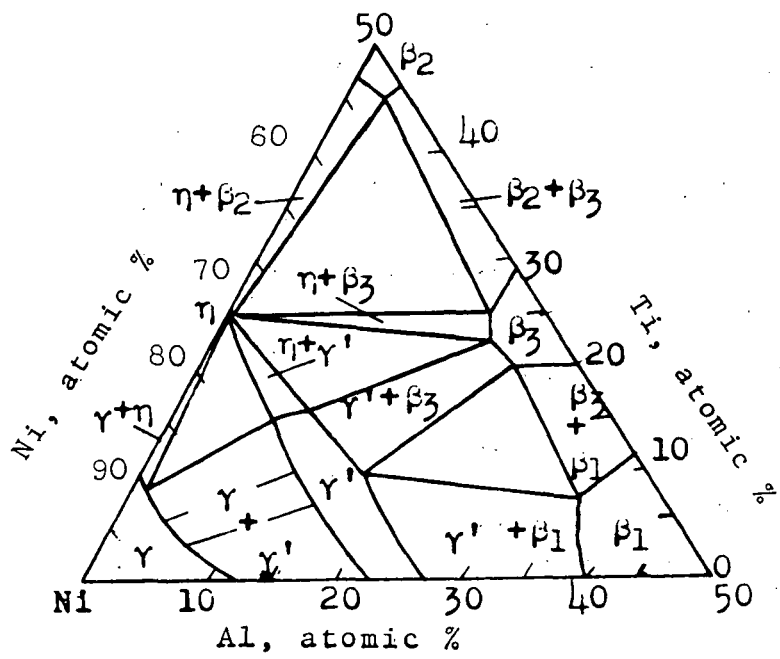


FIGURE 3 Ni-Ti-Al SYSTEM AT 750°C (ref. 10)

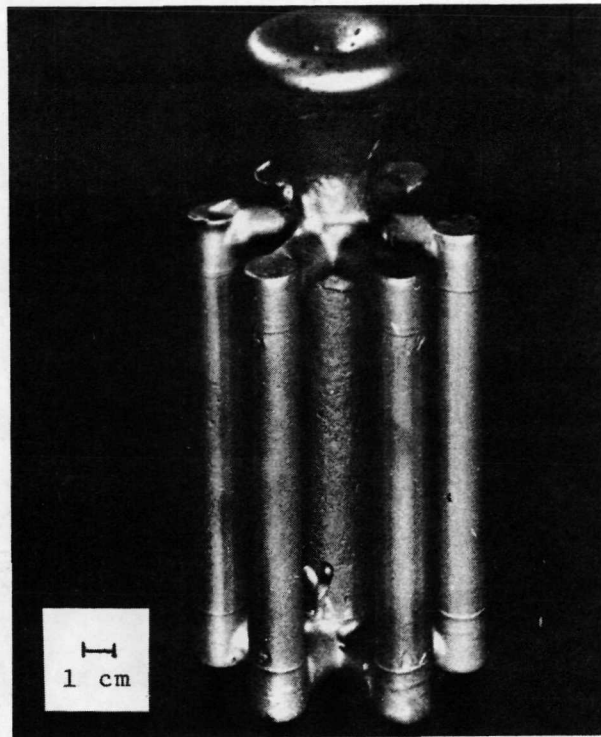
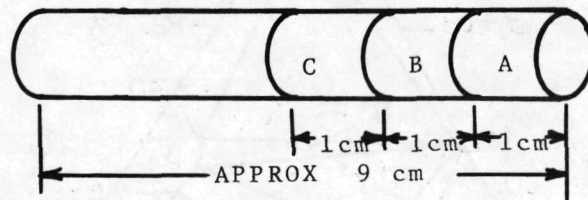


FIGURE 4 EXPERIMENTAL CASTING



- A - Metallography
- B - Extractions
- C - Chemical Analysis

FIGURE 5  
SPECIMEN LAYOUT

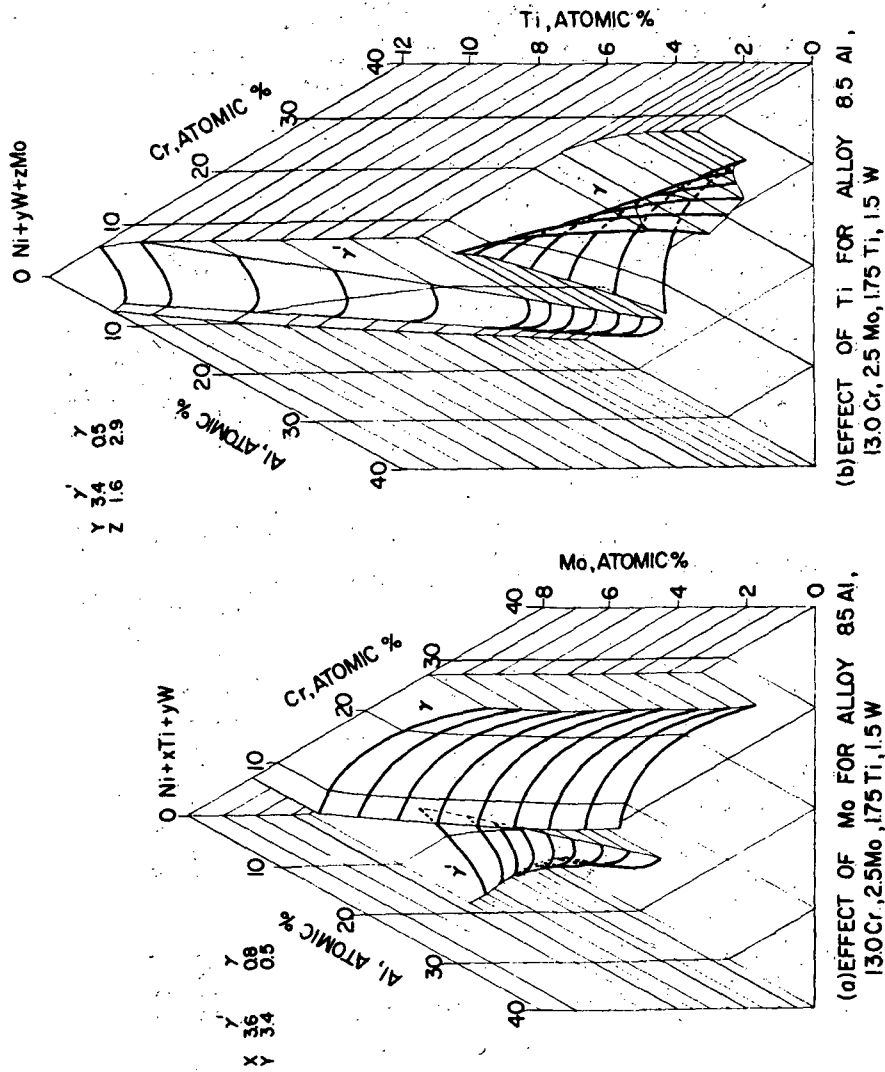
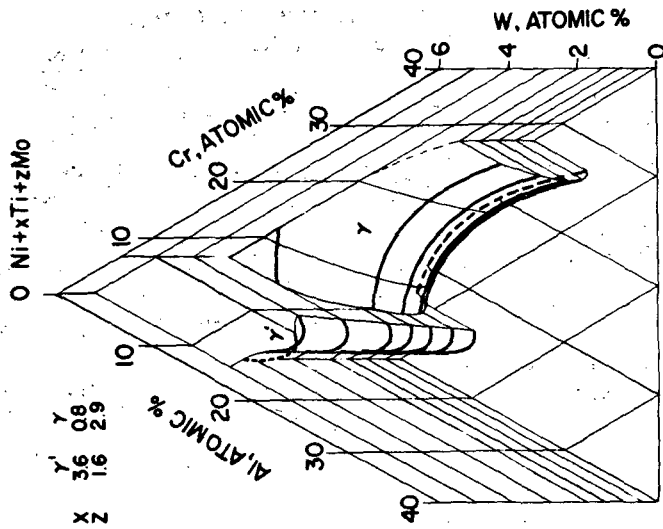
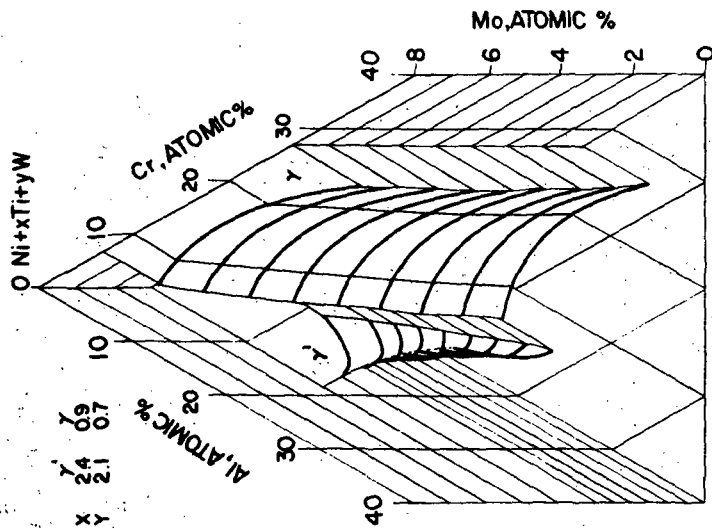


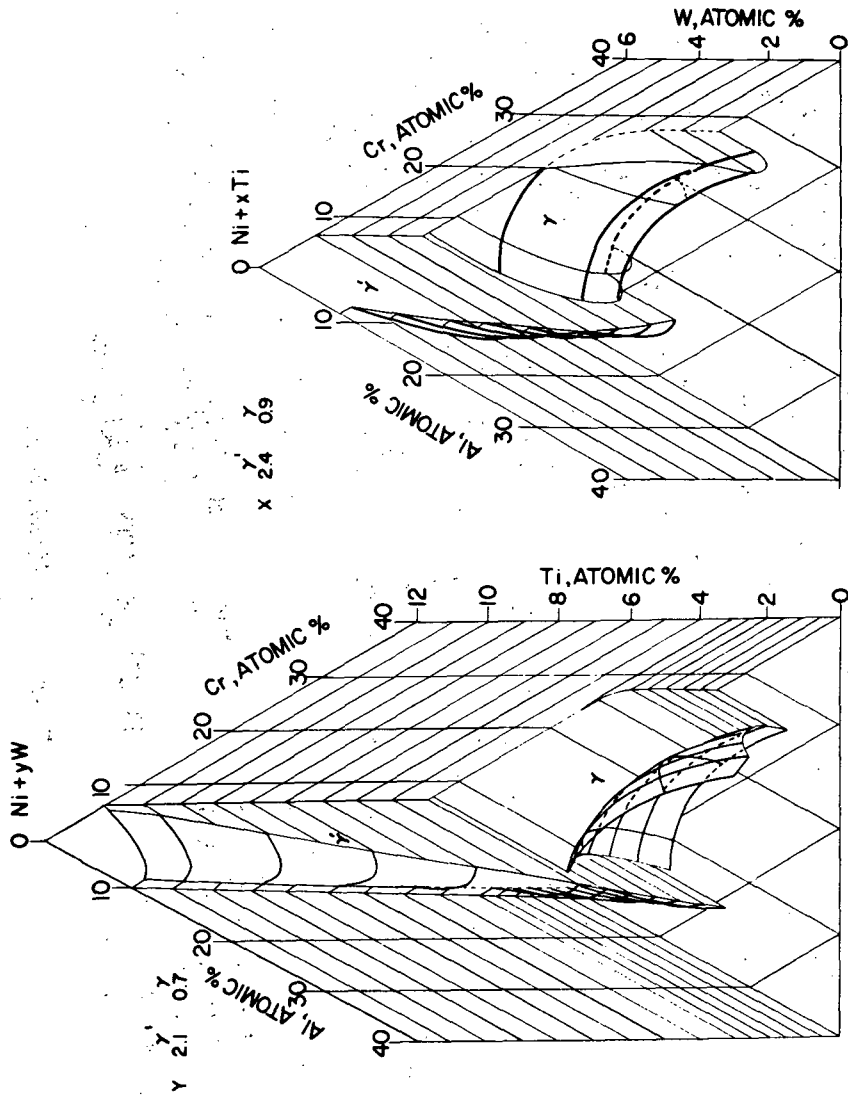
FIGURE 6 THE Ni-RICH REGION OF THE Ni-Cr-Al-Mo-Ti-W SYSTEM AT 850°C



(d) EFFECT OF Mo FOR ALLOY 85 Al, 13.0 Cr, 1.75 Ti, 1.5 W

(c) EFFECT OF W FOR ALLOY 85 Al, 13.0 Cr, 2.5 Mo, 1.75 Ti, 1.5 W

FIGURE 6 (CONTINUED)



(e) EFFECT OF Ti FOR ALLOY 85 Al, 130 Cr, 1.75 Ti, 1.5 W  
 (f) EFFECT OF W FOR ALLOY 85 Al, 130 Cr, 1.75 Ti, 1.5 W

FIGURE 6 (CONTINUED)



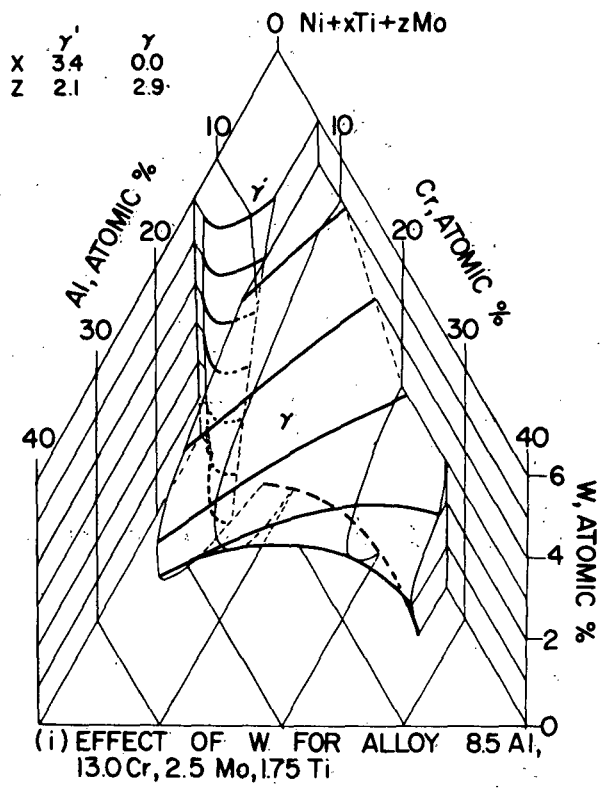
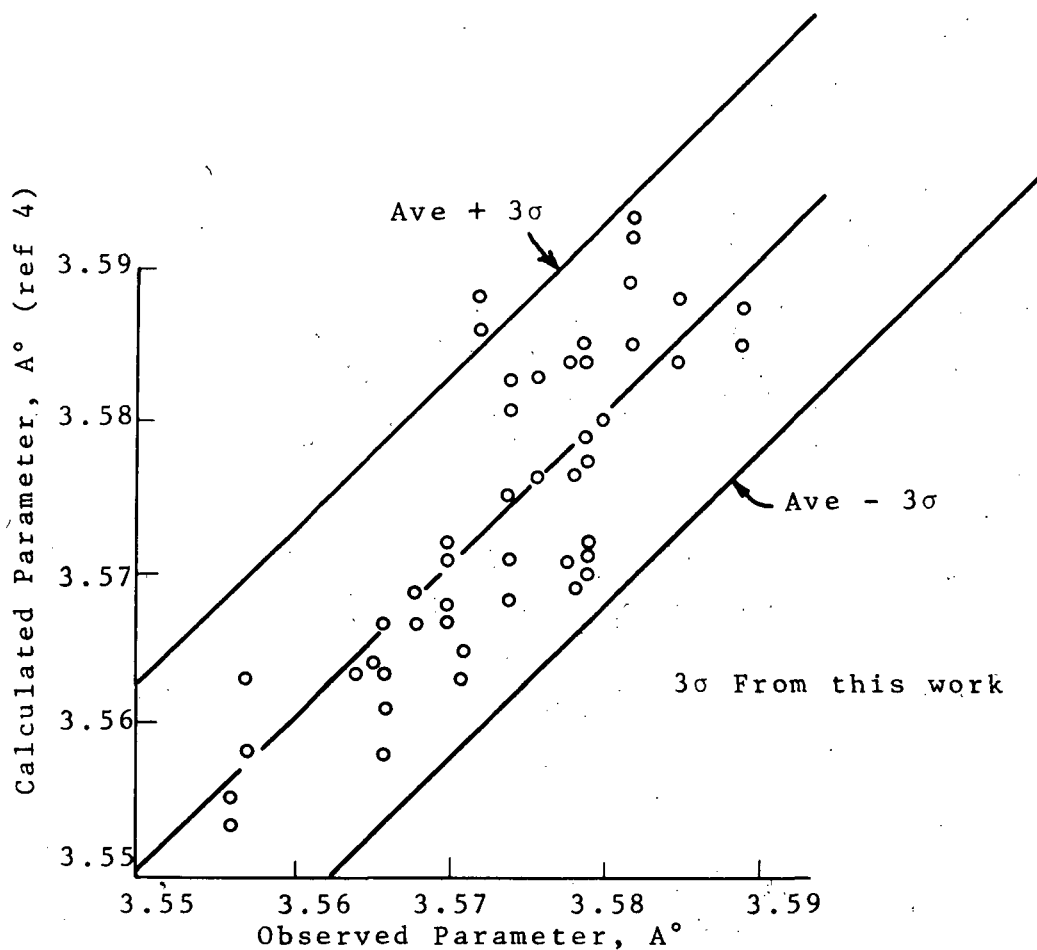
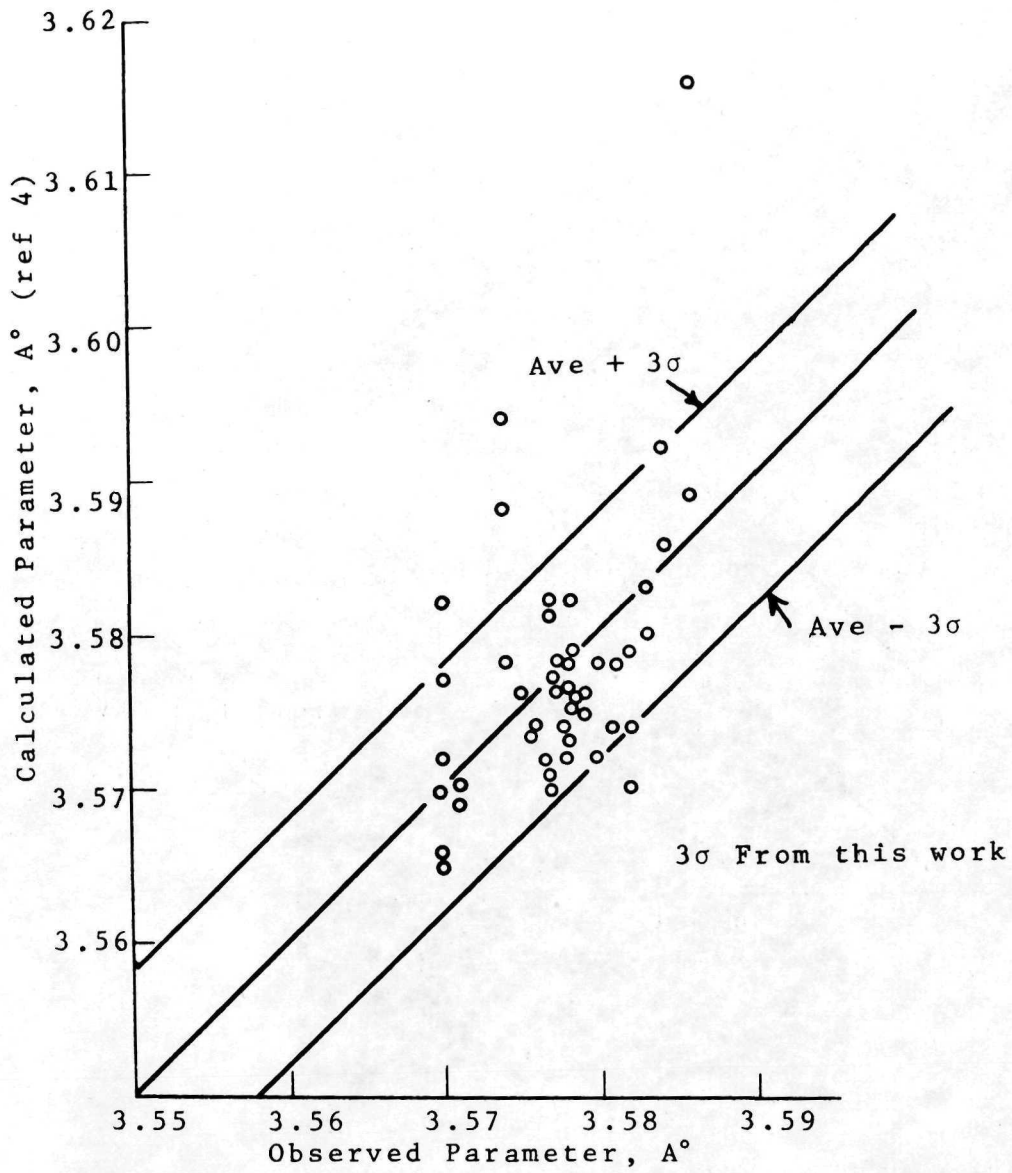


FIGURE 6 (CONCLUDED)



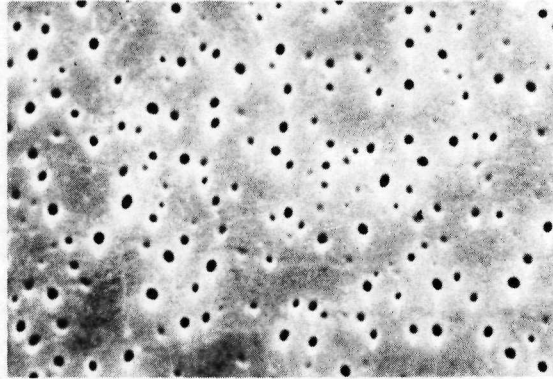
(a) Lattice Parameter of  $\gamma$

FIGURE 7 COMPARISON OF LATTICE PARAMETER ESTIMATION METHODS.



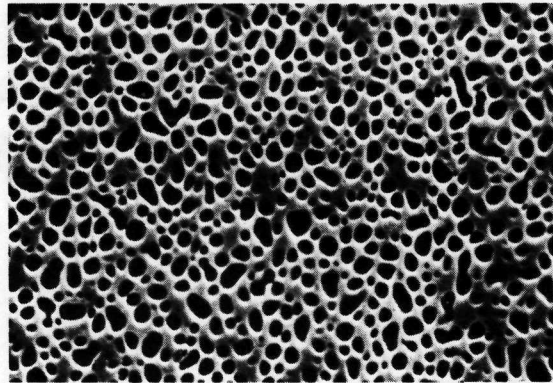
(b) Lattice Parameter of  $\gamma'$

FIGURE 7 (CONCLUDED)



(a) ALLOY 33 - ROUND  $\gamma'$

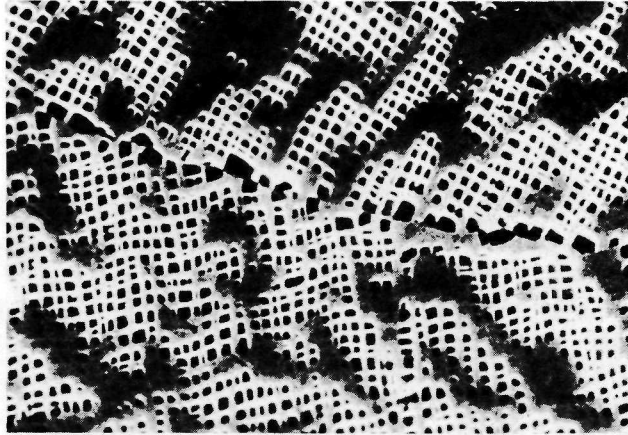
MAGNIFICATION: 10000



(b) ALLOY 39 - GLOBULAR  $\gamma'$

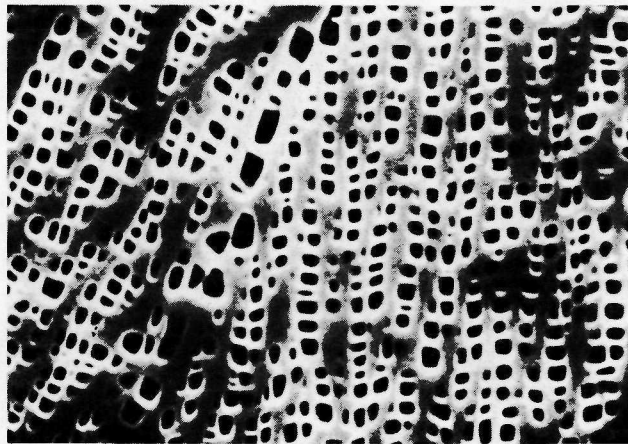
MAGNIFICATION: 5000

FIGURE 8 SCANNING ELECTRON MICROGRAPHS SHOWING  $\gamma$  AND  $\gamma'$   
MORPHOLOGIES ETCH: MIXED ACIDS



(c) ALLOY 99 - SQUARE  $\gamma'$

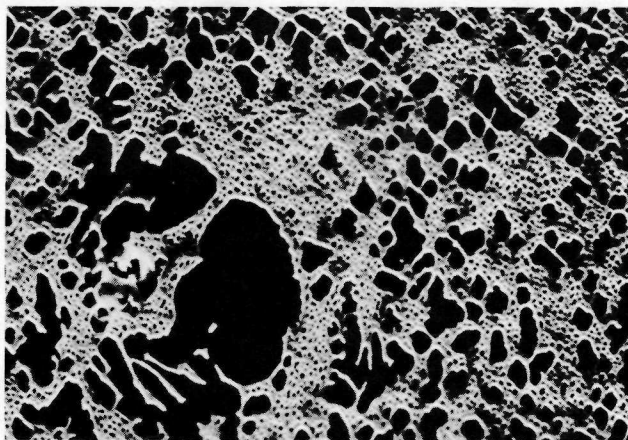
MAGNIFICATION: 5000



(d) ALLOY 37 - BLOCKY  $\gamma'$

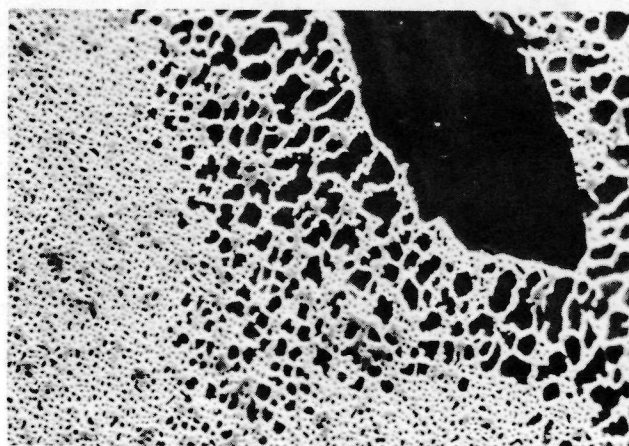
MAGNIFICATION: 10000

FIGURE 8 (CONTINUED)



(e) ALLOY 35 - PRIMARY  $\gamma'$

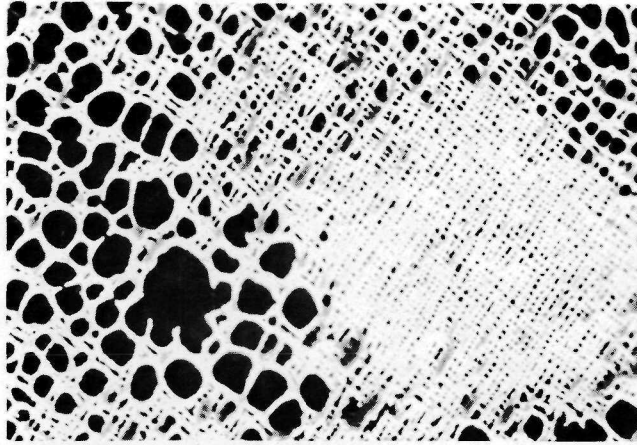
MAGNIFICATION: 2000



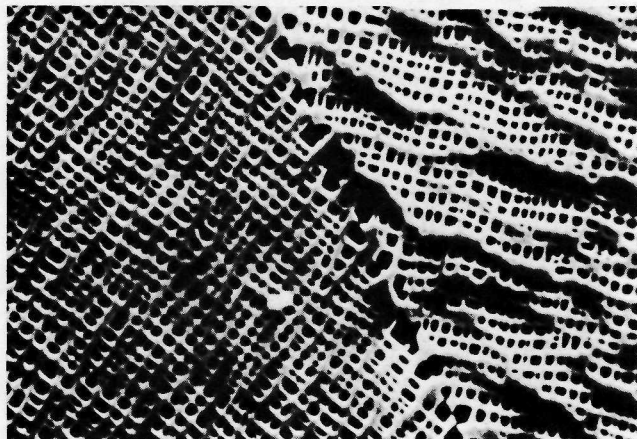
(f) ALLOY 40 - PRIMARY  $\gamma'$

MAGNIFICATION: 2000

FIGURE 8 (CONTINUED)

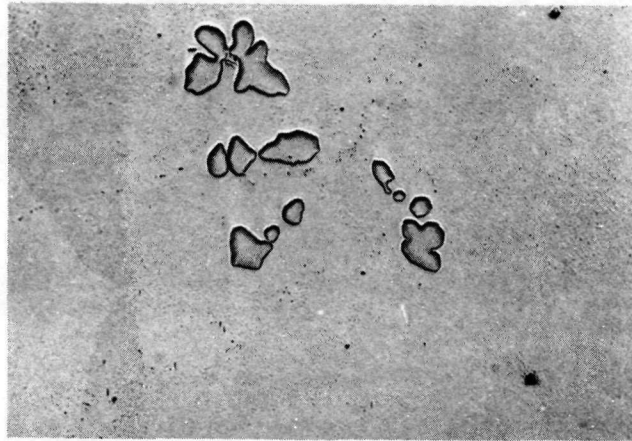


(g) ALLOY 7 - DUPLEX  $\gamma'$  SIZE      MAGNIFICATION: 2000



(h) ALLOY 7 - FINE-BLOCKY  $\gamma'$       MAGNIFICATION: 5000

FIGURE 8      (CONCLUDED)



(a) ALLOY 4 - W PHASE  
UNETCHED

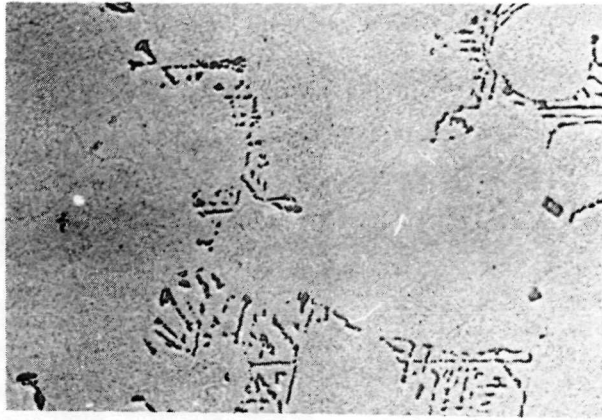
MAGNIFICATION: 250



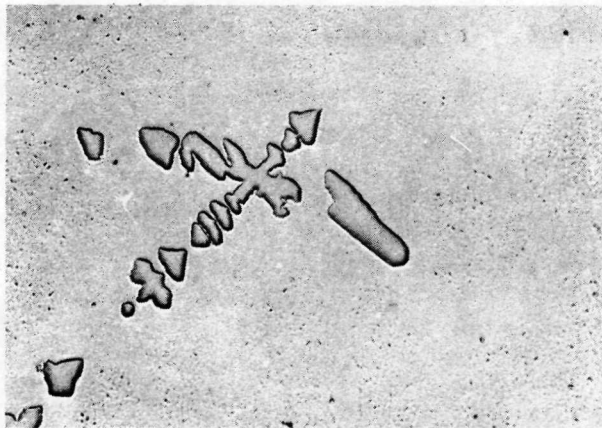
(b) ALLOY 6 - CHINESE SCRIPT W PHASE  
UNETCHED

MAGNIFICATION: 250

FIGURE 9 MICROGRAPHS SHOWING THE MORPHOLOGY OF PHASES  
OTHER THAN  $\gamma$  AND  $\gamma'$

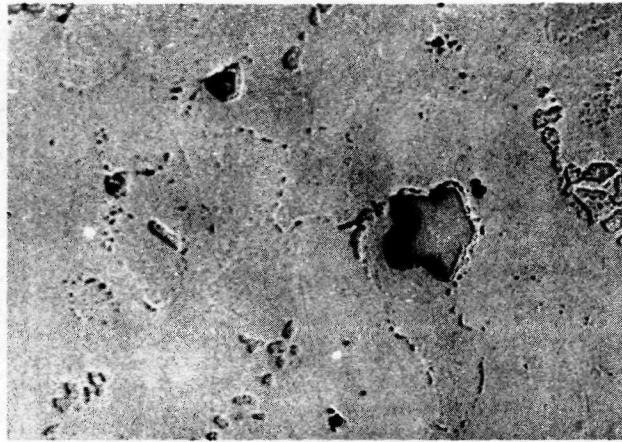


(c) ALLOY 10 - CHINESE SCRIPT W PHASE  
UNETCHED MAGNIFICATION: 250

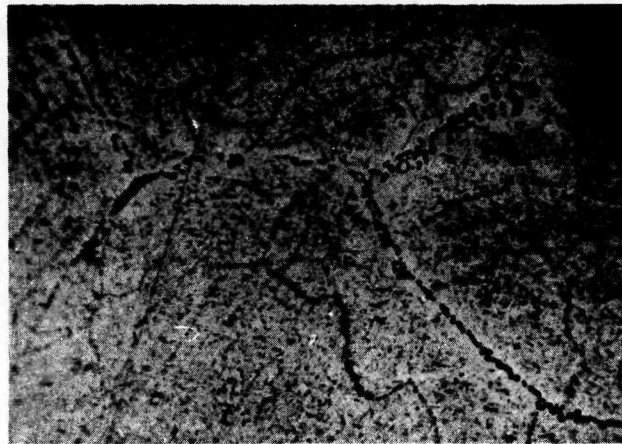


(d) ALLOY 25 - INTERDENDRITIC W PHASE  
UNETCHED MAGNIFICATION: 250

FIGURE 9 (CONTINUED)

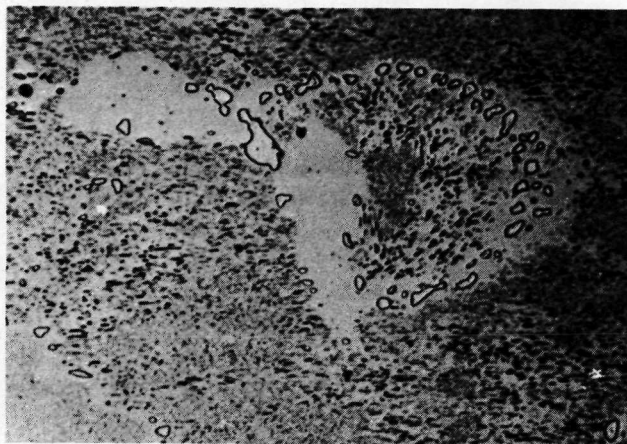


(e) ALLOY 8 - W PHASE WITH Cr RING  
ETCH: KOH MAGNIFICATION: 250



(f) ALLOY 17 - FINE Cr PHASE  
ETCH: KOH MAGNIFICATION: 500

FIGURE 9 (CONTINUED)



(g) ALLOY 24 - Cr PHASE  
ETCH: KOH

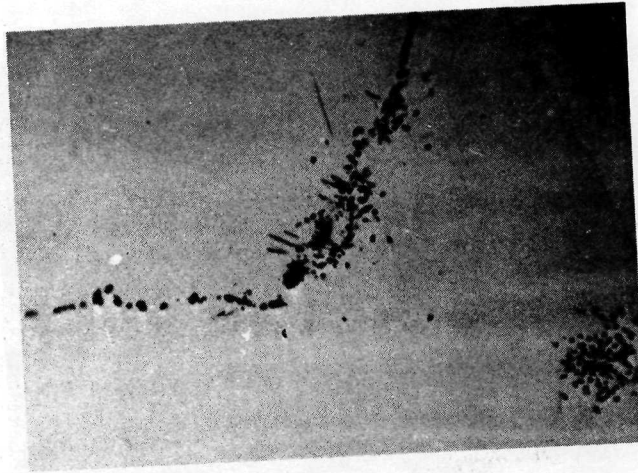
MAGNIFICATION: 750



(h) ALLOY 17 - Cr NEEDLES  
ETCH: MIXED ACIDS

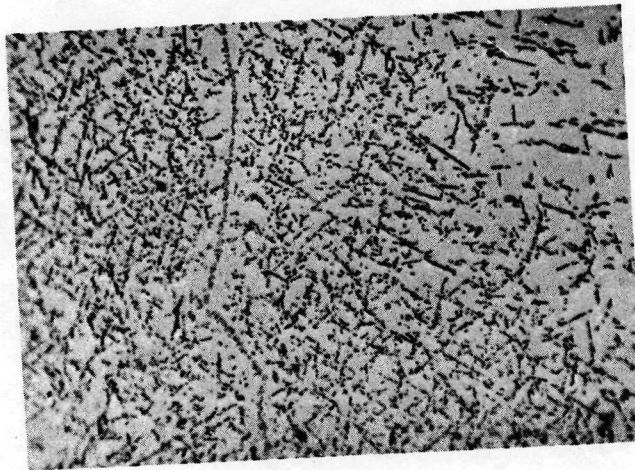
MAGNIFICATION: 5000

FIGURE 9 (CONTINUED)



(i) ALLOY 3 - Mu PHASE  
ETCH: KOH

MAGNIFICATION: 500



(j) ALLOY 13 - Mu PHASE  
ETCH: KOH

MAGNIFICATION: 500

FIGURE 9 (CONTINUED)



(k) ALLOY 6 - SIGMA AND W PHASES  
ETCH: KOH

MAGNIFICATION: 500

FIGURE 9 (CONCLUDED)

C

## APPENDIX

C

PROGRAM TO FIND GAMMA AND GAMMA PRIME COMPOSITION  
 THE INPUT IS IN ATOM PER CENT OF 2 PHASE ALLOY

C

C

THIS CONTAINS ONLY FIRST DEGREE TERMS FOR DIRECTION NUMBERS  
 REAL MO

DIMENSION TITLE(20)

1

WRITE(7,10)

10

FORMAT('0', 'AL CR MO TI W')

READ(5,20)AL,CR,MO,TI,W

READ(5,15)TITLE

15

FORMAT(20A4)

IF(AL.LE.001.AND.CR.LE..001.AND.TI.LE..001) GO TO 100

20

FORMAT(5(F5.2,1X))

C

CALCULATION OF DIRECTION NUMBERS

DAL=-2.4316+.0661\*AL+.05982\*CR+.008869\*MO+.1462\*TI+.09066\*W

IF(DAL.GT.0.) DAL=0.

DMO=-.003257-.001034\*AL-.01314\*CR+.08798\*MO+.0216\*TI+.0244\*W

IF(DMO.LT.0.) DMO=0.

DTI=-1.0469+.046595\*AL+.030941\*CR+.0267122\*MO-.070565\*TI+.040548\*W

IF(DTI.GT.0.)DTI=0.

DW=-.5284-.05424\*AL+.03004\*CR+.02086\*MO+.05451\*TI+.1403\*W

JK=0

L=0

LL=0

LLL=0

TAL=AL

TCR=CR

TMO=MO

TTI=TI

TW=W

N=0

A=.05

29

I=0

KK=0

J=0

NN=0

IF(AL.LE.0.) DAL=0.

IF(CR.LE.0.) DCR=0.

IF(MO.LE.0.) DMO=0.

IF(W.LE.0.) DW=0.

```

IF(DAL.GE.0.) GO TO 300
30 GO TO 50
40 CONTINUE

C GAMMA SURFACE

50 GAL=13.399-1.0739*TCR+1.8007*TMO+15.317*TW+.031851*TCR**2-.0455815
**TMO**2+1.5347*TTI**2-2.5987*TW**2-
*1.43936*TW*TMO*TTI+.153165*TTI*TCR*TMO+.48662
*5*TW*TCR*TTI-.100793*TCR*TMO-
*.204796*TCR*TTI-.504191*TCR*TW-2.12721*TMO*TTI+.598921*TMO*TW-7.75
*6*TTI*TW
IF(TAL.LE.0..AND.GAL.LE.0.) GO TO 70
TEST=TAL-GAL
ATEST=ABS(TEST)
IF(N.EQ.0) STEST=ATEST
IF(ATEST.LE.STEST.AND.ABS(A).GT..04.AND.TAL.GT..5) GO TO 21
GO TO 22
21 STEST=ATEST
SAL=TAL
SCR=TCR
STI=TTI
SMO=TMO
SW=TW
22 CONTINUE
IF(ATEST.LE..005)GO TO 70
IF(N.EQ.0)GO TO 55
IF (TEST)51,52,53
51 CONTINUE
IF(NN.EQ.-1) GO TO 70
IF(N.EQ.-1) GO TO 60
IF(A.GT.0..AND.NN.EQ.0) NN=1
IF(N.EQ.1) A=-.001
GO TO 60
52 GO TO 70
53 CONTINUE
IF(NN.EQ.1) GO TO 70
IF(N.EQ.1) GO TO 60
IF(A.GT.0..AND.NN.EQ.0) NN=-1
IF(N.EQ.-1) A=-.001
GO TO 60
55 CONTINUE
IF(TEST.GT.0.) N=1
IF(TEST.LT.0.) N=-1
IF(TEST.EQ.0.) GO TO 70
60 CONTINUE
IF(NN.EQ.0) I=0
IF(NN.NE.0) I=I+1

```

```

IF(I.GT.20000) GO TO 100
IF(LLL.EQ.1)LL=1
TCR=TCR+A
TAL=TAL+A*DAL
TMO=TMO+A*DMO
TTI=TTI+A*DTI
TW=TW+A*DW
IF(MO.EQ.0.)TMO=0.
IF(TI.EQ.0.)TTI=0.
IF(W.EQ.0.)TW=0.
IF(TCR.LE.0.)TCR=0.
IF(TMO.LE.0.)TMO=0.
IF(TTI.LE.0.)TTI=0.
IF(TW.LE.0.)TW=0.
IF(KK.EQ.1) GO TO 110
IF(TAL.LE.0.) TAL=0.
IF(TAL.LE.0..OR.TCR.GT.40.) GO TO 80
IF(TAL.GT.AL) GO TO 80
GO TO 40
70 CONTINUE
IF(JK.EQ.1) GO TO 71
WRITE(6,901)
901 FORMAT('-',)
WRITE(6,915) TITLE
915 FORMAT(1X,20A4)
WRITE(6,950)AL,CR,MO,TI,W
71 CONTINUE
IF(TAL.GT.0.) WRITE(6,995)TAL,TCR,TMO,TTI,TW
IF(JK.EQ.1) GO TO 81
IF(TAL.LE.0.)WRITE(6,995)SAL,SCR,SMO,STI,SW
995 FORMAT('0','GAMMA',T19,1X,5(F4.1,2X))
GO TO 81
80 CONTINUE
IF(JK.EQ.1) GO TO 81
WRITE(6,901)
WRITE(6,915) TITLE
WRITE(6,900)
WRITE(6,950) AL,CR,MO,TI,W
WRITE(6,995) SAL,SCR,SMO,STI,SW
81 CONTINUE
IF(JK.EQ.1) GO TO 101
T=TAL+TTI
IF(T.GT.9.) JK=1
IF(JK.EQ.1) N=0
IF(JK.EQ.1) NN=0
IF(JK.EQ.1) A=2.
IF(JK.EQ.1.AND.A.GT.1.9) GO TO 60
GO TO 101

```

```

900  FORMAT('0','THIS MAY BE SINGLE PHASE')
950  FORMAT('0',T21,'AL',T27,'CR',T33,'MO',T39,'TI',T45,'W'/'0','ALLOY'
    *,T13,
    *'AT PCT',1X,5(F5.2,1X))
101  CONTINUE
    KK=1
    NN=0
    TAL=AL
    TCR=CR
    TMO=MO
    TTI=TI
    TW=W
    A=-.05
110  CONTINUE
    IF(TAL.GT.30.OR.TCR.LE.0.) GO TO 210

C    GAMMA PRIME SURFACE

    GPAL=7.42647+3.59713*TCR+0.*TMO+.84906*TTI-.58923*TW-.292157*TCR**
    *2+.14993*TMO**2-.0256415*TTI**2
    *-.039818*TW**2-.12783*TCR*TMO-.31073*TCR*TTI+.29002*TCR*TW-.245979
    **TMO*TTI+.876515*TMO*TW
    *-.15534*TTI*TW+.0226054*TW*TMO*TTI-.275617*TW*TCR*TMO+.0675603*TTI
    **TCR*TMO-0.*TW*TCR*TTI
    TEST=TAL-GPAL
    ATEST=ABS(TEST)
    IF(J.EQ.0) STEST=ATEST
    IF(LLL.EQ.1.AND.A.LE.-.15.AND.J.EQ.0) GO TO 122
    IF(ATEST.LE.STEST) GO TO 121
    GO TO 122
121  STEST=ATEST
    SAL=TAL
    SCR=TCR
    STI=TTI
    SMO=TMO
    SW=TW
122  CONTINUE
    IF(J.EQ.0) GO TO 150
    IF(ATEST.LE..005) GO TO 200
    IF(TEST) 120,130,140
120  CONTINUE
    IF(J.EQ.-1)GO TO 60
    IF(A.LE.0..AND.NN.EQ.0) NN=1
    IF(NN.EQ.-1) GO TO 200
    IF(J.EQ.1) A=.001
    GO TO 60
130  GO TO 200
140  CONTINUE

```

```
IF(J.EQ.1) GO TO 60
IF(A.LE.0..AND.NN.EQ.0) NN=-1
IF(NN.EQ.1) GO TO 200
IF(J.EQ.-1) A=.001
GO TO 60
150 CONTINUE
IF(TEST.GT.0.) J=1
IF(TEST.EQ.0.) GO TO 200
IF(TEST.LT.0.) J=-1
GO TO 60
200 CONTINUE
WRITE(6,960)TAL,TCR,TMO,TTI,TW
TR=TCR+TMO+TW
IF(TR.GT.14..AND.LL.EQ.0) A=-5.
IF(TR.GT.14..AND.LL.EQ.0)NN=0
IF(TR.GT.14..AND.LL.EQ.0)LLL=1
IF(TR.GT.14..AND.LL.EQ.0)KK=1
IF(TR.GT.14..AND.LL.EQ.0) J=0
IF(TR.GT.14..AND.LL.EQ.0)GO TO 60
960 FORMAT('0','GAMMA PRIME',T19,1X,5(F4.1,2X))
GO TO 100
210 WRITE(6,960)SAL,SCR,SMD,STI,SW
WRITE(6,970)
GO TO 100
300 CONTINUE
WRITE(6,915)TITLE
WRITE(6,920)
WRITE(6,950)AL,CR,MO,TI,W
920 FORMAT('0','AL DIRECTION NUMBER IS 0. THE ALLOY IS UNSTABLE')
970 FORMAT('0','NO GAMMA PRIME INTERCEPT')
100 CONTINUE
GO TO 1
END
```

DISTRIBUTION LIST

No. of Copies	To
2	Library NASA Lewis Research Center 21000 Brookpark Road Cleveland, Ohio 44135
1	Patent Counsel NASA Lewis Research Center 21000 Brookpark Road Cleveland, Ohio 44135
1	Contracts Section B NASA Lewis Research Center 21000 Brookpark Road Cleveland, Ohio 44135
1	Report Control Office NASA Lewis Research Center 21000 Brookpark Road Cleveland, Ohio 44135
1	Technology Utilization NASA Lewis Research Center 21000 Brookpark Road Cleveland, Ohio 44135
40	National Technical Information Service Springfield, Va. 22151
2	NASA Scientific & Tech Information Facility Attn: NASA Rep Box 33 College Park, Md 20740
1	Library NASA Ames Research Center Moffett Field, California 94035
1	Library NASA Flight Research Center P.O. Box 273 Edward, California 93523

DISTRIBUTION LIST

No. of Copies	To
1	Library NASA Goddard Space Flight Center Greenbelt, Maryland 20771
1	Library Jet Propulsion Laboratory 4800 Oak Grove Drive Pasadena, California 91102
1	Library NASA Langley Research Center Langley Field, Virginia 23365
1	Library NASA Manned Space Flight Center Houston, Texas 77058
1	Library NASA Marshall Space Flight Center Huntsville, Alabama 35812
1	Deutsch, G.C./RW NASA Headquarters 600 Independence Ave. Washington, D.C. 20546
5	Mr. F.H. Harf NASA Lewis Research Center 21000 Brookpark Road Cleveland, Ohio 44135
1	Alexander, J.A. Materials Technology TRW Equipment Group 23555 Euclid Avenue Cleveland, Ohio 44117
1	Ault, G.M. 3-13 NASA - Lewis 21000 Brookpark Road Cleveland, Ohio 44135

DISTRIBUTION LIST

No. of Copies	To
1	Beck, J. Westinghouse Electric Co. Research Labs. Pittsburgh, Penna. 15235
1	Beattie, H J Bldg 55-103 General Electric 55 North Avenue Schenectady, New York 12305
3	Ashbrook RL 49-1 NASA Lewis Research Center 21000 Brookpark Road Cleveland, Ohio 44135
1	Barker, J.F. Bldg 500-M87 GE Company Cincinnati, Ohio 45215
1	Bieber, C. INCO Sterling Forest Suffern, New York 10901
1	Bliss, V. Climax Molybdenum Co. P.O. Box 1568 Ann Arbor, Michigan 48106
1	Boesch, W J Special Metals Inc. New Hartford, New York 13413
1	Canada, H B Special Metals New Hartford, New York 13413
1	Clarke, W Veletz Nuclear Center P.O. Box 846 Pleasanton, California 94566
1	Collins, Dr. H E Colwell Center TRW Inc. Cleveland, Ohio 44117

DISTRIBUTION LIST

No. of Copies	To
1	Couts, W H R + D Dept Wyman Gordon Co. N. Grafton, Mass. 01536
1	Cupp, C R INCO Sterling Forest Suffern, New York 10901
1	Danesi, W P Climax Molybdenum Co. 1600 Huron Pwy Ann Arbor, Michigan 48106
1	Danforth, A Mass Materials Research 55 Millbrook St. Worcester, Mass. 01606
1	Decker, Dr. Ray INCO Merica Research Lab. Suffern, New York 10901
1	Donachie, Dr. M J Pratt + Whitney Aircraft J Bldg - West Office East Hartford, Conn. 06108
1	Dreshfield, R L MS 49-1 Lewis Research Center 21000 Brookpark Road Cleveland, Ohio 44135
1	Eckel, Prof. Earl J 201 Met & Mining Bldg University of Illinois Urbana, Illinois 61803
1	Elbaum, J K AFML (MAMP) Wright-Patterson AFB Ohio 45433

DISTRIBUTION LIST

No. of Copies	To
1	Farrington, R J Bldg - West Office Pratt & Whitney Aircraft East Hartford, Ct. 06108
1	Freche J C MS 49-1 NASA - Lewis 21000 Brookpark Road Cleveland, Ohio 44135
1	Flowers, F C Allison Div General Motors Indianapolis, Indiana 46206
1	Gehlbach, Dr. R. Met. + Ceramics Div. Oak Ridge Natl Lab Bldg 4500-S Oak Ridge, Tenn. 37831
1	Geyer, N. AFML/LLP Headquarters Wright Patterson AFB Ohio 45433
1	Goldblatt Barry AVCO Lycoming Div. 550 S. Main St. Stratford, Ct. 06497
1	Green, D.R. Special Metals Corp. New Hartford, New York 13413
1	Hagel, W.C. Mtls Div. GE Company Cincinnati, Ohio 45215

DISTRIBUTION LIST

No. of Copies	To
1	Hamilton, P.E. Allison Div. General Motors Indianapolis, Indiana 46202
1	Hesse, Arlan A. Huntington Alloys Div. INCO Huntington, West Va. 25720
1	Hauser, A P&W A J Mezzanine E. Hartford, Ct. 06108
1	Hodge, F.G. Stellite Div. 1020 W. Park Avenue Kokomo, Ind. 46901
1	Isaacs, O.L. M-78 General Electric Co. Aircraft Engine GP Cincinnati, Ohio 45215
1	H Q Army Materials Comm. Attn: AMCRD-RS-CM Washington, D.C. 20360
1	Johnson, D. Battelle Memorial Inst. 505 King Avenue Columbus, Ohio 43201
1	Kaufman, Dr. M. General Electric Company Thompson Laboratory West Lynn, Mass. 01905
1	Kaufman, Dr. Larry Manlabs Inc. 21 Erie Street Cambridge, MA 02139

DISTRIBUTION LIST

No. of Copies	To
1	Kriege, Dr. O.H. J Bldg - West Office MERL Pratt & Whitney Aircraft E. Hartford, Ct. 06108
1	Lemkey, Dr. F.D. United Aircraft Corp. Research Laboratories East Hartford, Ct. 06108
1	Kotval, Dr. P. RIAS Martin Marietta Corp. 1450 South Rolling Road Baltimore, Md 21227
1	Levy, I.S. Battelle Memorial Inst. Pacific N W Labs Richland, Va. 99352
1	Lherbier, L.W. Universal Cyclops Steel 650 Washington Road Pittsburgh, Penna. 15228
1	Lund, Carl Martin Metals 250 North Twelfth St. Wheeling, Illinois 60090
1	Maniar, G.N. Research Lab. Carpenter Steel Company Reading, Penna. 19603
1	Maxwell, D. International Nickel Company One New York Plaza New York, New York 10004
1	MCIC Battelle Memorial Inst. 505 King Avenue Columbus, Ohio 43201

DISTRIBUTION LIST

No. of Copies	To
1	Mihalisin, Dr. J.R. INCO Research Lab. Sterling Forest Suffern, New York 10901
1	Moon, Dr. D.M. Westinghouse Corp. Research Laboratories Pittsburgh, Penns. 15235
1	Miner, Dr. R.V. Jr. MS 49-1 Lewis Research Center 21000 Brookpark Road Cleveland, Ohio 44135
1	Moore, J.B. Pratt + Whitney Aircraft Box 2691 West Palm Beach, Florida 33402
1	Mrdjenovich, R. Turbine Operations Ford Motor Company 2000 Rotunda Drive Dearborn, Michigan 48183
1	Muzyka, Dr. D.R. Carpenter Steel P.O. Box 662 Reading, Penna. 19603
1	Newkirk, Dr. J.B. Dept. of Metallurgy University of Denver Denver, Colorado 80210
1	Nichols, E.S. Allison Div. of G M Indianapolis, In 46206
1	Nail, D. Camercon Iron Wks P.O. Box 1212 Houston, Texas 77001

DISTRIBUTION LIST

No. of Copies	To
1	Probst, Dr. H.B. MS-49-1 NASA Lewis Research Center 21000 Brookpark Road Cleveland, Ohio 44135
1	Omara, E.F. Committee E4 ASTM Revere Copper Inc. Rome, New York 13441
1	Pierce, Dr. C.M. AFML MAMP WPAFB Ohio 45433
1	Pitcairn D. Amsted Industries Research Lab. 340 County Line Road Bensenville, Illinois 60106
1	Quigg R. J. VP + GNL Mgr. Jetshapes Inc. Rockleigh Industrial Park Rockleigh, New Jersey 07647
1	Radavich, Dr. J.F. Micro Met. Inc. Box 3074 W. Lafayette, Indiana 47906
1	Raymond, E.L. Huntington Div. International Nickel Company Huntington, W. Va. 25720
1	Sims., C.T. Bldg 55-213 General Electric Company 55 North Avenue Schenectady, New York 12305
1	Smith, R.L. J Bldg Pratt + Whitney Aircraft East Hartford, Conn. 06108

DISTRIBUTION LIST

No. of Copies	To
1	Sponseller, Dr. D.L. Res. Lab. Climax Moly Company 1600 Huron Pkway Ann Arbor, Michigan 48106
1	Stickler, Dr. R. Westinghouse Research Lab. Rue Gatta De Gamond 95 1180 Brussels, Belgium
1	Stroup, J.P. Latrobe Steel Company Latrobe, Pennsylvania 15620
1	Sullivan, Dr. C.P. CDS-MERL Pratt + Whitney Aircraft East Hartford, Ct. 06108
1	Varin, J.C. Ford Motor Company 2000 Routunda Drive Dearborn, Michigan 48124
1	Tarshis, Dr. L.A. General Electric Company R. & D. Center P.O. Box 8 Schenectady, New York 12301
1	Veil, E.I. PWA MDL-B08 P.O. Box 2691 West Palm Beach, Florida 33402
1	Wall, F.J. Steam Div. Westinghouse P.O. Box 9175 Lester, Penna. 19113
1	Wilcox, Dr. Ben A. Battelle Memorial Inst. 505 King Avenue Columbus, Ohio 43201

DISTRIBUTION LIST

No. of Copies	To
1	Wilson, Dr. D. Department of Metallurgy University of Michigan Ann Arbor, Michigan 48104
1	Wlodek, Dr. S.T. Stellite Division Cabot Corporation 1020 W. Park Avenue Kokomo, In. 46901
1	Woody Att L.R. Homer Res. Laboratories Bethelam, Penna. 18016